A STUDY OF THE EFFECT OF SINUSOIDAL VIBRATIONS UPON THE MEASUREMENT OF THERMAL CONDUCTIVITY OF DISTILLED WATER

By

PAUL WILLIAM MONTGOMERY

Bachelor of Science
Wichita State University
Wichita, Kansas
1960

Master of Science
Oklahoma State University
Stillwater, Oklahoma
1963

Submitted to the Faculty of the Graduate School
of the Oklahoma State University
in partial fulfillment of the requirements
for the degree of
DOCTOR OF PHILOSOPHY
July, 1968

A STUDY OF THE EFFECT OF SINUSOIDAL VIBRATIONS UPON THE MEASUREMENT OF THERMAL CONDUCTIVITY OF DISTILLED WATER

Thesis Approved:

E. L. Doughty
Thesis Adviser

R. L. Lowery

J. R. Morton

N. N. Durham
Dean of the Graduate College

PREFACE

The purpose of this study was to determine the effect of sinusoidal vibrations upon the measured values of thermal conductivity of distilled water. The scope of the study included determining the effect of various frequencies and forces of acceleration upon samples of distilled water.

The author wishes to express his sincere thanks and to acknowledge his indebtedness to many people for their role in the completion of this study.

Particular appreciation is expressed to Dr. J. A. Wiebelt and Dr. R. L. Lowery for patience, technical guidance, and encouragement. Appreciation is also expressed to other members of the committee, Dr. E. T. Dowty and Dr. O. H. Hamilton.

The author is also indebted to technicians of the AF Aero Propulsion Laboratory, Mr. Harry E. Jones of the Plasma Dynamics Technical Area and Mr. William Smith of the Instrument Shop.

Mrs. Annette Powell and Miss Barrie Lubart are thanked for the typing of the final manuscript.

TABLE OF CONTENTS

Chapter		Page
I.	INTRODUCTION	1
	Statement of the Problem	1
	The Purpose and Scope of the Study	2
	Previous Work	2
II.	DESCRIPTION OF TEST APPARATUS	8
	Design Criteria	8
	Test Chamber	9
	Vibration Equipment	13
	Thermocouples	17
	Instrumentation	24
III.	DETERMINATION OF THERMAL CONDUCTIVITY	33
	Introduction	33
	Calculation of Q_{IN} (Heat Applied)	34
	Calculation of Q_L (Heat Loss)	36
	Calculation of R_O, R_T, and K_L	48
	Maximum Uncertainty	49
IV.	METHOD AND PROCEDURE	53
	Test Procedure	53
	Sample Calculation	55
V.	TEST RESULTS AND CORRELATIONS	58
	Experimental Data	58
	Visible Phenomena	69
	Comparison of Data	69
VI.	CONCLUSIONS AND RECOMMENDATIONS	71
	Recommendations for Future Study	71
A SELECTED BIBLIOGRAPHY		73

Chapter Page

APPENDIX 75

A. List of Symbols. 75
B. List of Major Instrumentation. 77
C. Calibration of Thermocouples 79
D. Instrumentation Error for Calculation of Maximum Uncertainty 91
E. Computer Program - Thermocouple Calibration. . . . 95
F. Computer Program - Regression Program (Sum of Least Squares) 97
G. Computer Program - Calculation of E_0, E_T, Q(Corrected), Thermal Conductivity K_L, and Maximum Uncertainty from Observed Date 101

LIST OF TABLES

Table		Page
I.	A Summary of Eight Outstanding Investigators and Their Apparatus Used In Measurement of the Thermal Conductivity of Water, Since 1900.	5
II.	Calculation of Q(L).	39
III.	Comparison of Data	70
IV.	Thermocouple Calibration Data.	85

LIST OF FIGURES

Figure		Page
1.	Thermal Conductivity of Water - A Summary of Work since 1900.	6
2.	Test Chamber.	10
3.	Test Apparatus Assembled.	14
4.	Components of Test Chamber.	15
5.	Vibration Equipment	16
6.	Typical Thermocouple Schematic.	19
7.	Thermocouple Placements	21
8.	Thermocouple Circuit for the Measurement of Hot Plate Bottom Temperature (HPBT)	22
9.	Thermocouple Circuit for the Measurement of Cold Plate Temperature (CPLT).	23
10.	Circuit for the Measurement of Top Plate Guard Temperature (TPGT) and Hot Plate Top Temperature (HPTT)	25
11.	Circuit for the Measurement of Hot Plate Top Temperature (HPTT), Hot Plate Bottom Temperature (HPBT), and Hot Plate Guard Temperature (HPGT).	26
12.	Assembly.	27
13.	Schematic for Measurement of Heat Supplied (QIN).	29
14.	Instrumentation Inside Screen Room.	31
15.	Instrumentation Outside Screen Room	32
16.	Modes of Heat Transfer.	37
17.	Values of R_0 Versus Frequency	59
18.	K_F/K_S Versus Frequency for Film Thickness of 0.600 Inches . .	61

Figure Page

19. K_F/K_S Versus Frequency for Film Thickness of 0.500 Inches. 62

20. K_F/K_S Versus Frequency for Film Thickness of 0.400 Inches. 63

21. K_F/K_S Versus Frequency for Film Thickness of 0.300 Inches. 64

22. K_F/K_S Versus Frequency for Film Thickness of 0.200 Inches. 66

23. K_F/K_S Versus Frequency for Film Thickness of 0.100 Inches. 67

24. K_F/K_S Versus Frequency for Film Thickness of 0.600 with Variable G Force 68

CHAPTER I

INTRODUCTION

Many industrial processes involve heat transfer through a liquid medium. These same processes are usually subjected to a vibrational environment due to the presence of pumps, compressors, etc. A previous investigator, while determining values of the thermal conductivity of liquids under static conditions, noted a significant departure from static values occurred when the test apparatus was subjected to small vibrations. Much work has been done investigating the effect of vibration upon the convection heat transfer coefficient as it relates to the perturbations of the boundary layer. However, it appears that little or no consideration has been given to the apparent influence of vibration upon the thermal conductivity of liquids. In view of this, a basic study of this phenomena and the associated mechanism is needed.

Statement of the Problem

The problem is to determine if vibration does indeed have an effect upon the measured values of thermal conductivity of water. It is also of importance to determine the influence of independent parameters and the magnitude of influence as they are allowed to vary independently. It is also of importance to investigate the mechanism that produces this phenomena and to determine if the phenomena is actually visible, as reported by a previous investigator.

The Purpose and Scope of the Study

This investigation was conducted using a thermoconductiometric apparatus with a horizontal film of circular cross section. The apparatus is very similar to standard horizontal film laboratory apparatus for measuring values of thermal conductivity of liquids. The film thickness could be varied from 0.100 inches to 0.600 inches in increments of 0.10 inches. The frequency was varied from 0-300 cycles per second, using the following increments: 0, 6.5, 8.0, 10.0, 12.0, 14.0, 16.0, 18.0, 20, 40, 60, 80, 100, 200, and 300 cycles per second for each increment of film thickness. The liquid bulk temperature was held constant at 93°F, and the liquid sample was heated downward to preclude convective flow. The amplitude of the vibrating motion was adjusted with each frequency to maintain an acceleration of 1.0 G (RMS value).

As a consequence of this investigation, the measured values of thermal conductivity was found to increase from five percent to eleven percent, in the frequency range of 6.5 to 14.0 cycles per second. The frequency of maximum response was determined to be a function of film thickness.

Previous Work

A literature search was made for the thermal conductivity of liquids to determine the methods used to measure the thermal conductivity of liquids, the comparative accuracies of such methods, and effects of vibrations on thermal conductivity. The literature was surveyed through May 1967.

The survey was divided into three parts. Part one was a compilation of the methods and apparatus used to measure thermal conductivity of liquids. Part two was a comparison of data on thermal conductivity of liquids by previous investigators, since 1900, to aid in forming a comparison with data derived from this study. Part three was a summary of work on the effect of vibrations upon the thermal conductivity of liquids.

Part 1

Summaries of earlier investigators, as reported by Mason (1) have been made by Jacob (2), Smith (3), Eucken (4), and Riedel (5).

In the past twenty years, five basic shapes of apparatus have been used by investigators; the thin horizontal film, the thick horizontal layer, the small diameter cylinder, the large diameter cylinder, and the thin film spherical type device.

Kardos (6) used a silver tube 1.6 mm in length in which a 0.1 mm diameter platinum wire was stretched along the axis. Heat was supplied by an electrical current in the wire and the wire temperature was computed from the electrical resistance. The heat flows radially outward from the wire to the tube, which is mounted vertically in a thermostatically controlled bath. Hutchinson (7) used a similar device which employed a 1.0 cm pyrex tube and an 0.088 mm tungsten wire. Stalhane and Pyk (8) used a wire stretched vertically in a large diameter cylindrical container. This apparatus depends upon the transient response to sudden heating of the wire. Pfriem (9) used basically the same method. Weishaupt (10) used a glass tube 6 cm in diameter

which contained a gold wire 0.07 mm in diameter. Van der Held and Van Drunen (11) used a similar device with a 0.3 mm manganin heater and thermocouple encased in a glass capillary.

Martin and Lang (12) used an apparatus designed to embody a thin circular film of liquid, 1.07 mm thick with downward heating. Riedel (5) used a similar device except the heating element was shrouded in a 1 mm film of liquid. Bates et al (13) used a similar arrangement except a thick film adjustable from 0.125 to 4 inches was used. The device used guard heaters and downward heating. Temperatures were measured by thermocouples immersed directly in the liquid sample.

Bridgman (14), Smith (15), and Daniloff (16) used a short cylindrical heater cylinder 0.375 inches in diameter which was surrounded by a test liquid layer 0.016 inches thick and 1.25 inches long. The ends were closed off with German-Silver foil.

Schmitt and Sellschopp (17) used the annular film arrangement with a test layer 30 mm x 120 mm x 0.5 mm. H. L. Mason (1) also used the annular film arrangement but used a relatively long test apparatus which measured 0.16 inches thick, 0.3743 inches diameter and 5 inches long. He used nonmetallic closures and fine lead-in wires to reduce the thermal end effects.

Schrock and Starkman (18) used a spherical steady state apparatus. In this apparatus the test sample is held between concentric copper spheres, and the temperature differential was determined by embedding differential thermocouples in the inner surfaces of the outer sphere and the outer surfaces of the inner sphere. This spherical apparatus does not require guard heaters, to attain adiabatic ends and edges as do apparatus of other geometry.

Part II

To facilitate comparison of data for the thermal conductivity of water, Table 1 and Figure 1 are given. Table 1 shows the summary of eight outstanding investigators, and types of apparatus used since 1900. Figure 1 shows a summary of their work with thermal conductivity plotted as a function of temperature.

TABLE I

A SUMMARY OF EIGHT OUTSTANDING INVESTIGATORS AND THEIR APPARATUS USED IN MEASUREMENT OF THE THERMAL CONDUCTIVITY OF WATER SINCE 1900

CURVE NO.	INVESTIGATOR(S)	YEAR	TYPE APPARATUS
1	Jacob	1920	Thin Horizontal Film
2	Martin and Lang	1933	Thin Horizontal Film
3	Weishaupt	1940	Large Diameter Tube
4	Bates and Hazzard	1945	Thick Horizontal Film
5	Van der Held and Van Drunen	1949	Large Diameter Tube
6	Riedel	1951	Large Diameter Tube
7	Gillam and Lamm	1955	Large Diameter Tube
8	Challoner and Powell	1956	Thick Horizontal Film

The purpose of this preliminary investigation was to determine if a correlation existed between the types of apparatus used and the measured values of thermal conductivity. The apparatus shown in Table I and the measured values given in Figure 1 failed to disclose any such correlation.

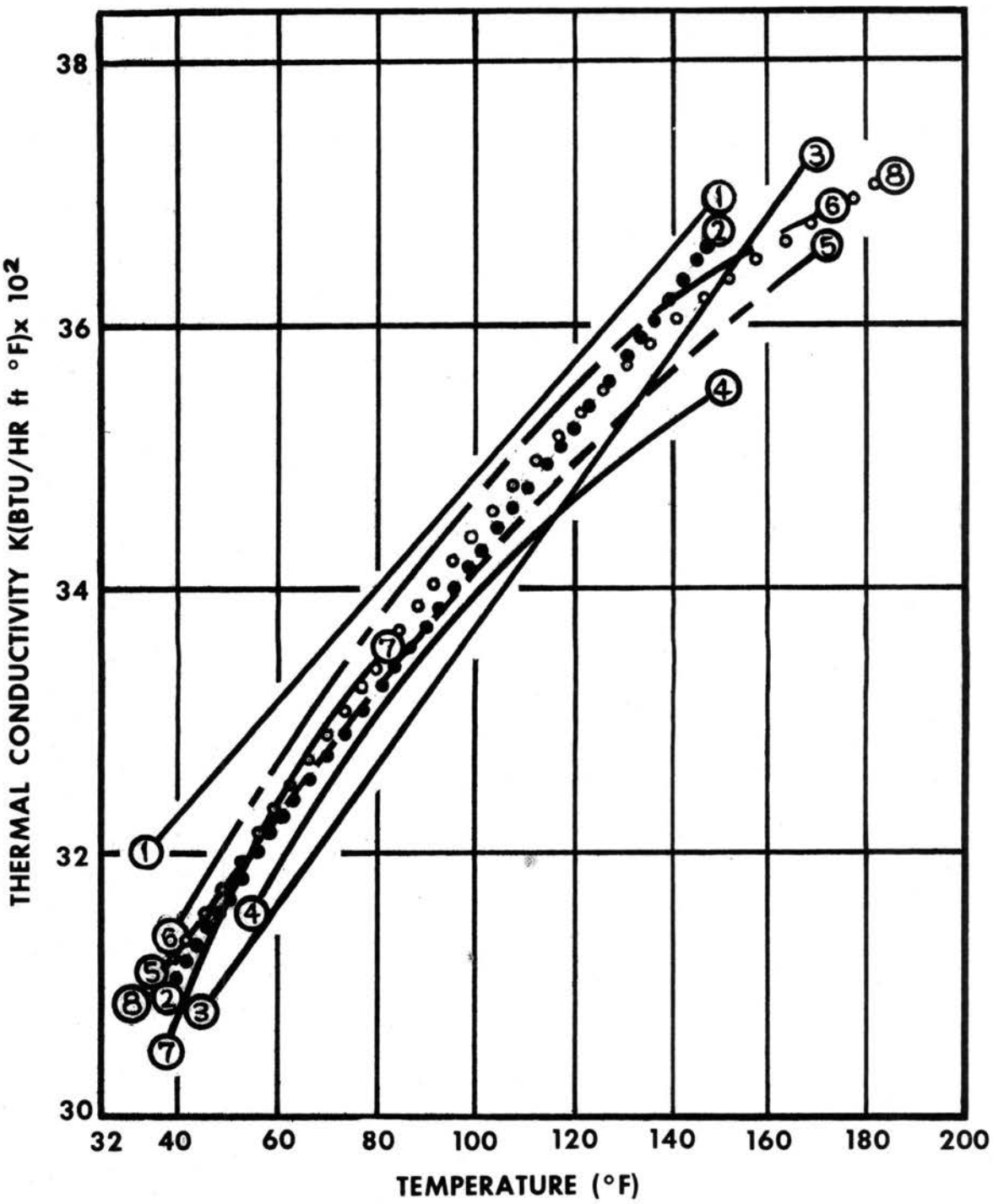

FIGURE 1- THERMAL CONDUCTIVITY OF WATER-

A SUMMARY OF WORK SINCE 1900

Part III

An exhaustive literature survey failed to disclose any previous work in this specific area, although much work has been directed toward investigating the effects of vibration on convective heat transfer due to perturbation in the boundary layer. Also, vibrations have been imparted to the heating element and an oscillatory motion generated relative to the heat transmitting medium.

A previous investigator (19) noted quite by accident that mechanical vibrations imposed on a horizontal thick film apparatus produced a significant departure from static values of thermal conductivity. Since his investigation was directed solely toward determining values of thermal conductivity, he immediately isolated his equipment from such effects and noted this phenomena in a report. Upon closer questioning, his personal observations included a visible phenomena within the liquid sample under the influence of vibration, which he described as follows:

> We made no measurement of thermal conductivity under conditions in which we thought that this vibration has any noticeable effect on the accuracy of our measurements. In those cases in which this effect was observed, it was manifested by a very peculiar motion within the test layer. Where vibration occurred, it was manifested by what appeared to be small elements of fluid marching very much as a column of soldiers would march across the surface of the test cell. We were unable to explain why this phenomenon should have manifested itself in this manner.

It was within the following frame of reference that this investigation was begun: Static values of thermal conductivity as determined by the recognized investigators on one hand, and on the other hand a significant departure from static values when influenced by a vibrating environment.

CHAPTER II

DESCRIPTION OF TEST APPARATUS

Design Criteria

The basic equation for thermal conductivity of a liquid, designated K_L, is given as

$$K_L = Q\ \Delta X / A\ \Delta T.$$

ΔT is the temperature differential across the sample thickness ΔX, and Q is the quantity of heat transferred over an effective Area A.

Therefore, in designing a test apparatus for the specific purpose of measuring the apparent effect of vibrations on the thermal conductivity of liquids, the following considerations must be given:

a. An accurate measurement of temperature differential (ΔT) must be made.

b. The liquid film thickness (ΔX) must be measured accurately.

c. The effective area of heat transfer (A) must be accurately determined.

d. The heat flow (Q) must be measured accurately.

e. Heat loss should be reduced to a minimum by proper design, and correction made for the minimal.

f. Convection effects due to temperature gradient should be studied and eliminated.

g. The metal surfaces should be parallel, smooth, plane, and

isothermal.

h. The liquid layer should be clearly visible at all times to detect the presence of bubbles, the possible occurrence of visible phenomena, and possible convection effects associated with the vibrational mode.

i. The vibration mode must be accurately controlled as to frequency, wave form, acceleration, and a minimum of horizontal component.

j. Heat transfer by radiation between the heater element and adjacent guard surfaces and through the liquid sample should be considered.

k. Precise thermal guarding should be employed to reduce heat loss to a minimum.

l. The vibrational mode must not change the physical constraints of the liquid sample, nor introduce unwanted influences, such as cavitation.

The consideration to be given paramount importance was to design a test apparatus that would fulfill the criteria outlined above, provide a minimum of error, and yet provide a means of calculating this minimum of error. As a measure of success, the possible error of each function was calculated as well as the maximum deviation in the determination of thermal conductivity.

Test Chamber

The test chamber, as shown in Figure 2, was designed to fulfill the above criteria and consists of a heater element, a top plate guard, guard heaters, plastic test chamber, fused silica spacers, cold plate, and water spray chamber.

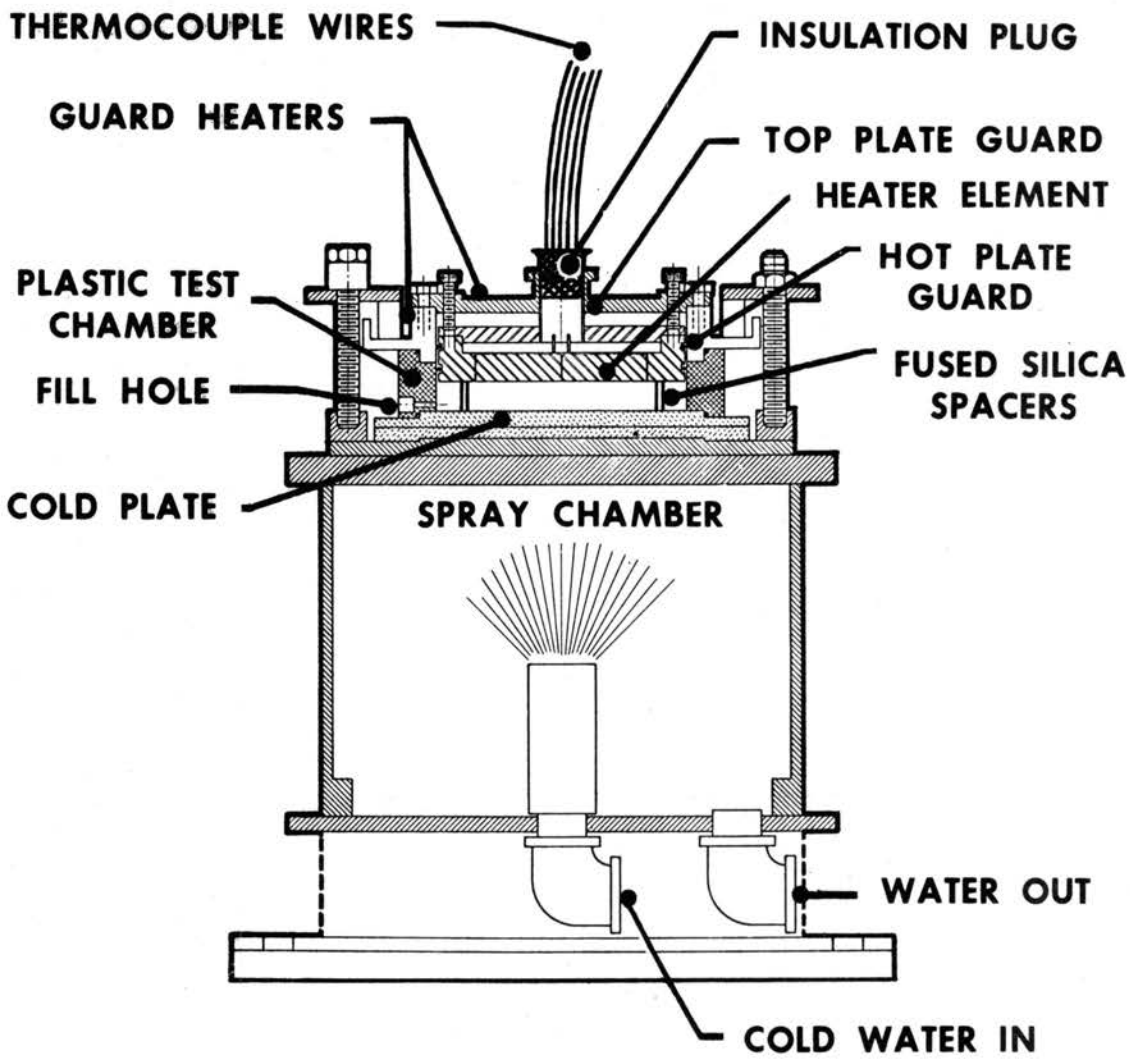

FIGURE 2- TEST CHAMBER ASSEMBLY

The heater element was machined from commercially pure, grade 100, copper to provide isothermal conditions. A silicone rubber heater element was cemented to the inside cavity. The resistance wiring was spiralled within the heater element to provide equal heat distribution. O-ring grooves on the side walls provide sealing for the liquid sample in the test chamber. The bottom surface was carefully machined, planed, lapped flat, chromium plated, and polished to a high lustre mirror finish. The chromium finish was used to reduce radiation and prevent deterioration of the pure liquid sample.

The side walls of the heater element were also chromium plated and O-rings were placed in the peripheral grooves. An O-ring material was chosen that offered maximum inertness and is commonly used in food processing machinery to avoid any possible contamination.

A stainless steel, type 304, centering bushing prevents misalignment of the heater element and permits physical extraction. The centering tube was purposely constructed of a very thin wall section and relatively low thermal conductivity (K = 7.76) to minimize heat transfer.

The top surface was machined and buffed to a high lustre to minimize radiant heat transfer.

The outer ring, designated the Hot Plate Guard, was machined from commercially pure aluminum and polished to a high lustre on the inside. The Hot Plate Guard provides thermal guarding for the heater element, which minimizes the heat transfer in the radial direction and provides support for the test chamber. The upper cover designated the Top Plate Guard also provides thermal guarding, and minimizes heat transfer in the vertical direction. It was machined from commercially

pure copper, and its inside surface was machined and buffed to a mirror-like finish to minimize radiative heat losses. A silicone rubber heater element was attached to the top surface. The heating element was especially designed to withstand vibration, and provide uniform heat distribution. The hold down screws, stainless steel, type 304, prevent displacement of the heater element during vibration, and maintain an accurate and constant film thickness. The hold down screws, No. 10, were bored out to an inside diameter of 0.125 inches. The resulting effective cross-sectional area was minimum. A clear plastic circular ring of low thermal conductivity (K = 0.12) provides a means of viewing the liquid sample during test, and permits detection of bubble formation, and the occurrence of visible phenomena. A small fill hole 0.10 inches in diameter permits filling the chamber and small vent holes 0.040 inches in diameter on the opposite side, permits the entrapped air to escape.

The bottom plate of the test chamber was machined of commercially pure copper, grade 100. It was honed, lapped flat, chromium plated and buffed to a mirror finish.

The film thickness of the liquid sample was accurately maintained by three fused silica spacers, of circular cross-section. The three spacers were cut from circular fused silica rod, ends machined to the exact dimensions of the desired film thicknesses, and measured with micrometer accuracy of $\pm$0.0005 inches. The utmost care was used to maintain accuracy of the film thickness.

Four clamping screws hold the test chamber rigidly to the spray chamber. Four insulating blocks restrain the outer ring, designated Hot Plate Guard.

The assembled test chamber was mounted on a spray chamber. A spray nozzle, located within the spray chamber uniformly sprays the entire bottom surface, which in turn cools the copper bottom plate. The spray water was removed by an outlet in the bottom of the spray chamber. The assembled test chamber and spray chamber are shown in Figure 3, and the components are shown disassembled in Figure 4.

Vibration Equipment

The vibration equipment schematic, as shown in Figure 5, consists of the following:

a. Two motor generator field exciter sets, bed mounted (Calidyne Model No. 45B-100-1)

b. Control console (Calidyne Model 45A)

c. Vibration table (Calidyne Model 44)

d. Instrumentation which includes:

1. Accelerometers (2)
2. Charge amplifier
3. Calibrated coaxial cables
4. Vacuum tube millivolt meter
5. EPUT meter
6. Oscilloscope

The motor generator field exciter set provided excitation to the field coil of the shaker table for two frequency ranges, "low" and "high." The low frequency range was 0-125 CPS and the high frequency was 0-500 CPS. The frequency of excitation is controlled by the armature current powerstat on the face of the control console panel.

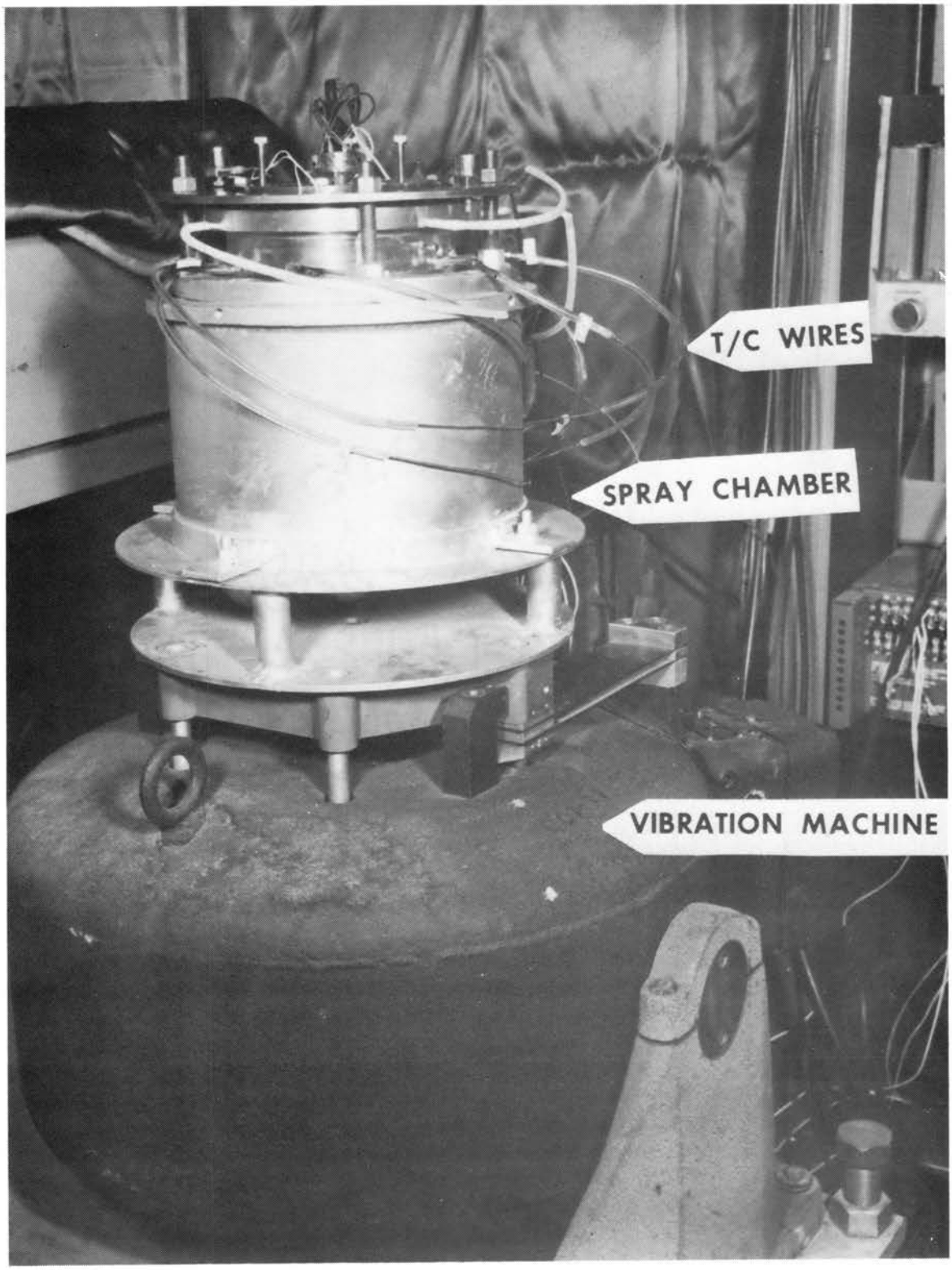

FIGURE 3- TEST APPARATUS ASSEMBLED

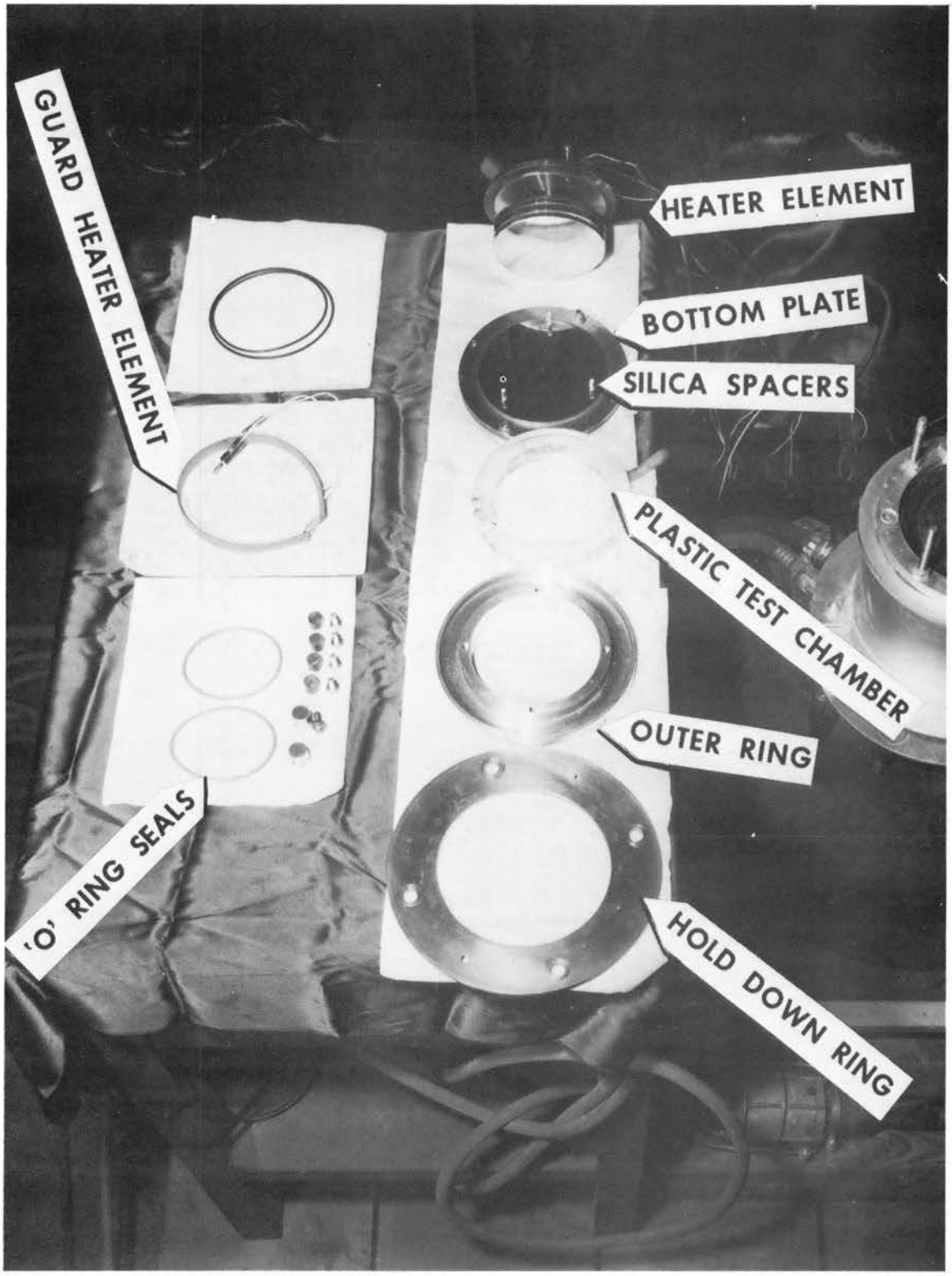

FIGURE 4- COMPONENTS OF TEST CHAMBER

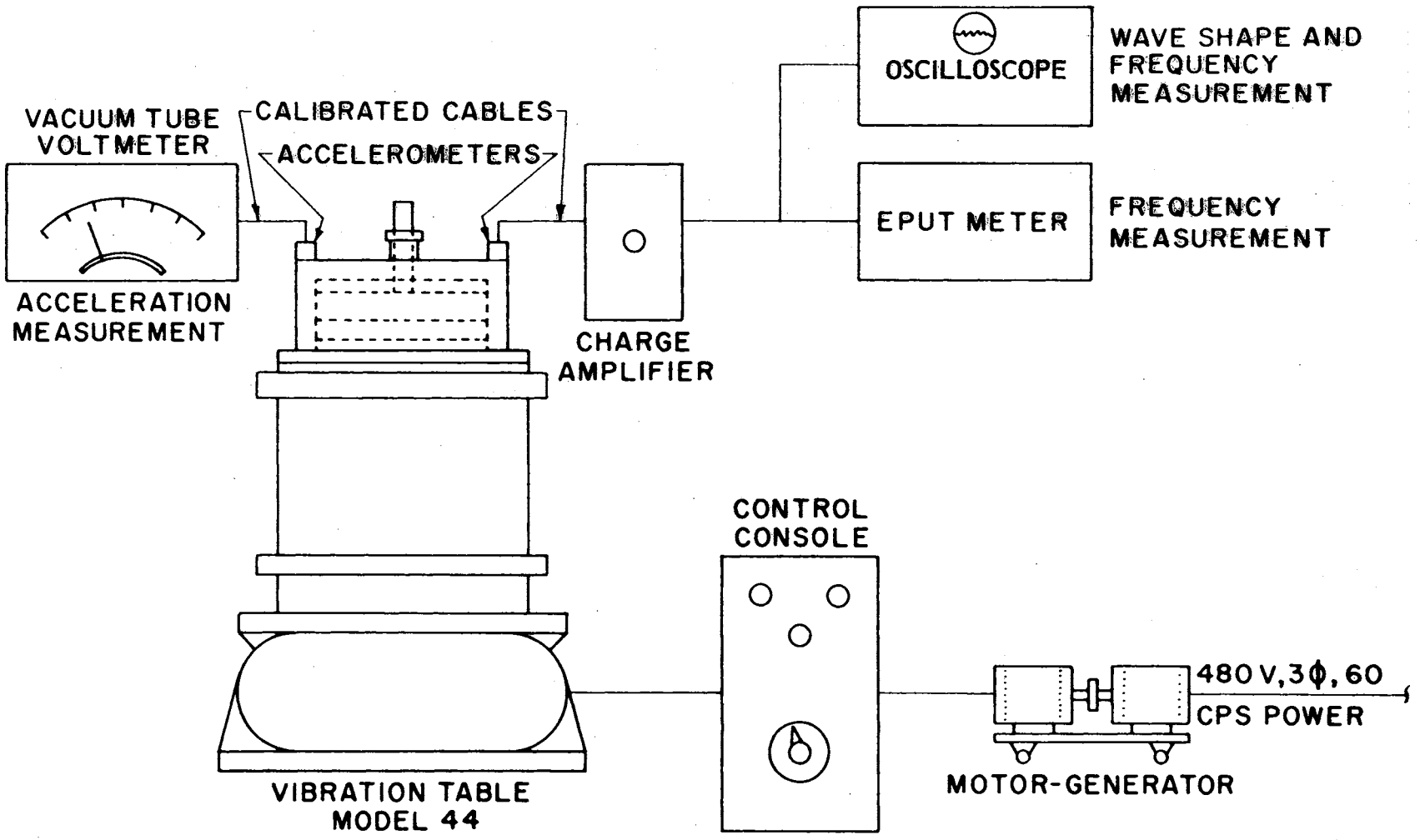

FIGURE 5- VIBRATION EQUIPMENT

The accelerometers mounted on the test chamber act as transducers to measure frequency and acceleration and display the corresponding wave shape on the oscilloscope.

The EPUT meter measured vibration frequency and the millivolt meter indicates acceleration in millivolts.

The accelerometer used to measure force level was calibrated against a NASA (National Aeronautics and Space Administration) standard accelerometer which was calibrated by the National Bureau of Standards.

All major instrumentation is listed in Appendix B. The associated accuracy and the standard against which the calibration was made is given in Appendix D.

Thermocouples

The accurate determination of thermal conductivity is predicated upon the ability to accurately determine temperature at remote locations and yet not influence other parameters, such as area, heat transfer, etc. The necessity to accurately measure temperature under conditions influenced by vibrations, yet with minimum disturbance of the surface dictates the use of calibrated thermocouples. The employment of thermocouples was considered most crucial in this investigation and considerable attention was directed toward their proper calibration and integration into the test apparatus. The following discussion relates the calibration procedure, the results, the placement of the individual thermocouples in the test apparatus and the associated instrumentation.

All thermocouples were fabricated from a single spool of copper-constantan wire purchased from the Honeywell Regulator Company. The thermocouple wire was cut in five foot lengths and at the end of each length the thermocouple element was formed. The ends were bared with fine sandpaper, twisted gently and carefully soldered. Great care was taken to insure cleanliness of wires and a minimum of solder used. A special preparation of resin flux solder was used to avoid the possibility of acids or alkalies. The twisted section was then carefully sanded until the tubular joint did not exceed 0.020 inches in length. This was done to provide the most uniform temperature along the longitudinal axis of the thermocouple junction.

The thermocouple elements were connected in series, eight in a group, and six groups. In each group, four thermocouples were used for reference temperature and four for temperature measurement. A thermocouple schematic of a typical group is shown in Figure 6.

Calibration was conducted as outlined in Appendix C. As a result of that calibration the following conclusions were made:

a. A high degree of homogeneity existed in the thermocouples.

b. Accuracy of $\pm 0.035^{\circ}F$ could be expected from thermocouples of Groups 3 and 4, for temperatures up to $150^{\circ}F$.

c. Accuracy of $\pm 0.063^{\circ}F$ could be expected from thermocouples of Groups 1, 2, 5 and 6, for the entire temperature range.

d. The reference temperature (ice point) was exact. The mean deviation of all thermocouples from standard curve was zero.

e. Thermocouples of Groups 3 and 4 would be used to measure temperature difference across the liquid sample where greatest accuracy is required. Thermocouples of Groups 1, 2, 5, and 6 would be used

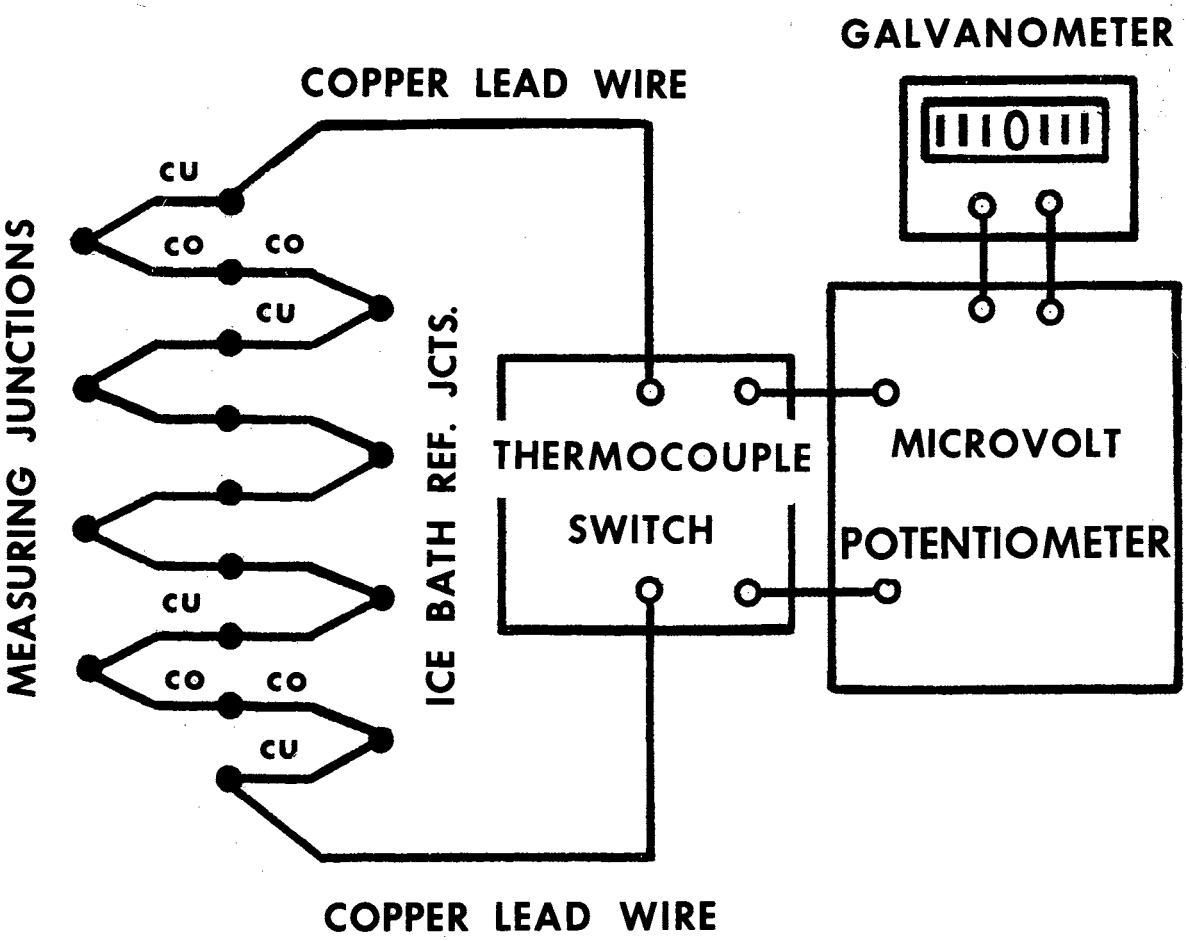

FIGURE 6- TYPICAL THERMOCOUPLE SCHEMATIC

to measure temperatures where less accuracy would be acceptable.

Thermocouples from Group 3 were used to measure the Hot Plate Bottom Temperature (HPBT) and those from Group 4 were used to measure Cold Plate Temperature (CPLT). The installation in the heater element was made by drilling holes 0.040 inches in diameter in the face, perpendicular to the surface. The thermocouple bead was placed even with the surface and the hole filled with an inert thermal-setting plastic. The inside surface of the heater element was grooved to allow the thermocouple wires to pass horizontally under the heater element in a near isothermal environment before exiting vertically through the center bushing. Care was taken to insure the thermocouple wires were well insulated, and did not contact either the heater element or the incoming lead wires. A similar installation was made by placing thermocouples in the cold plate. Here, again the thermocouple wires were extracted horizontally to afford as near isothermal conditions as possible. Thermocouples were placed in the top of the heater element to determine the Hot Plate Top Temperature (HPTT). Thermocouples were placed in identical fashion in the inner surface of the Top Plate Guard. Thermocouples were also placed at a 90 degree spacing on the circumference of the Hot Plate Guard inner surface, as shown in Figure 7.

The thermocouple schematic for measurement of Hot Plate Bottom Temperature (HPBT) and Cold Plate Temperature (CPLT) are shown in Figures 8 and 9. The thermopile arrangement allowed the reference junction and the measuring junctions to be connected using copper-copper and constantan-constantan junctions exclusively. This precludes the possibility of spurious emfs being generated by joining dissimilar

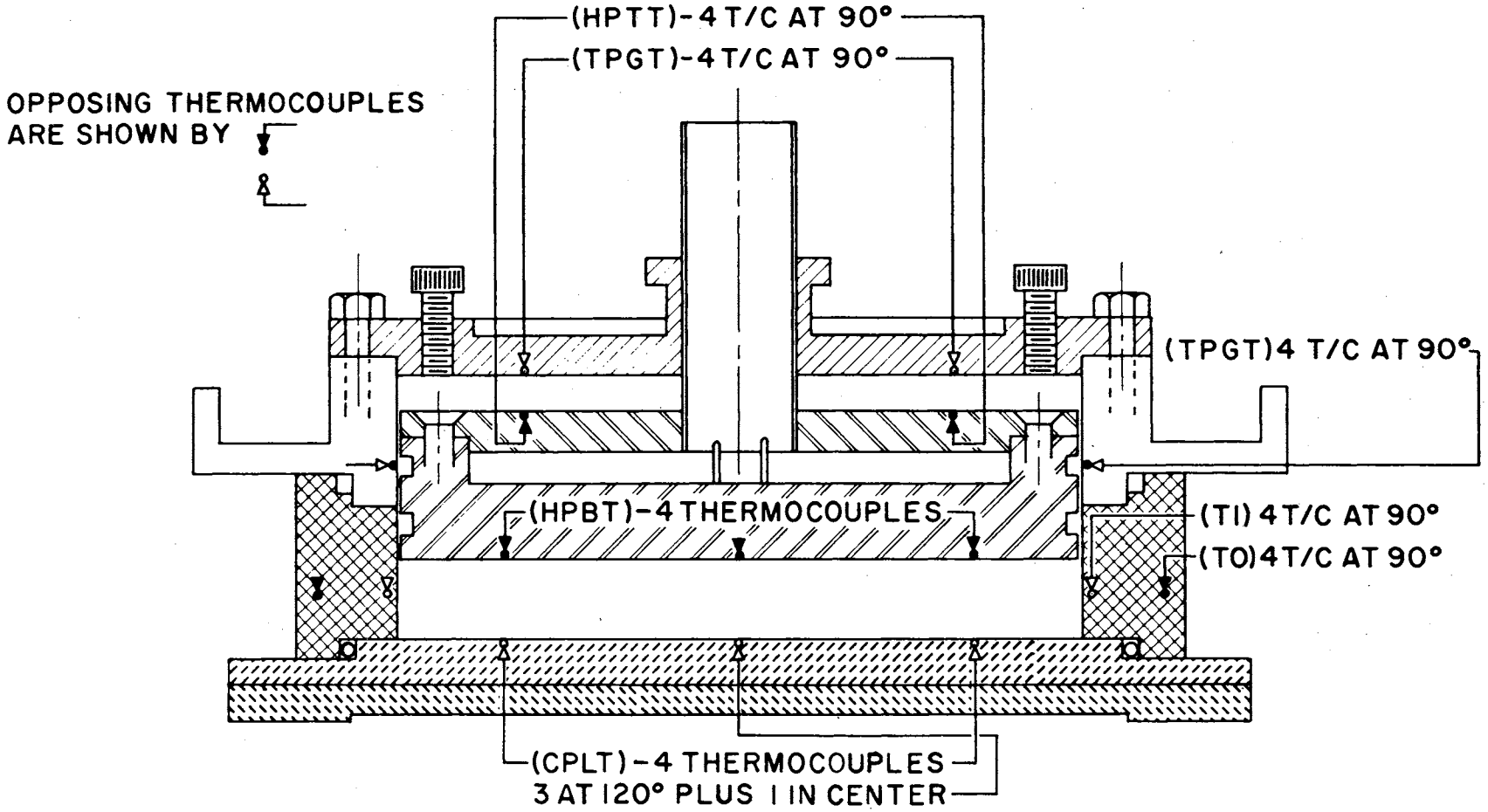

FIGURE 7- THERMOCOUPLE PLACEMENTS

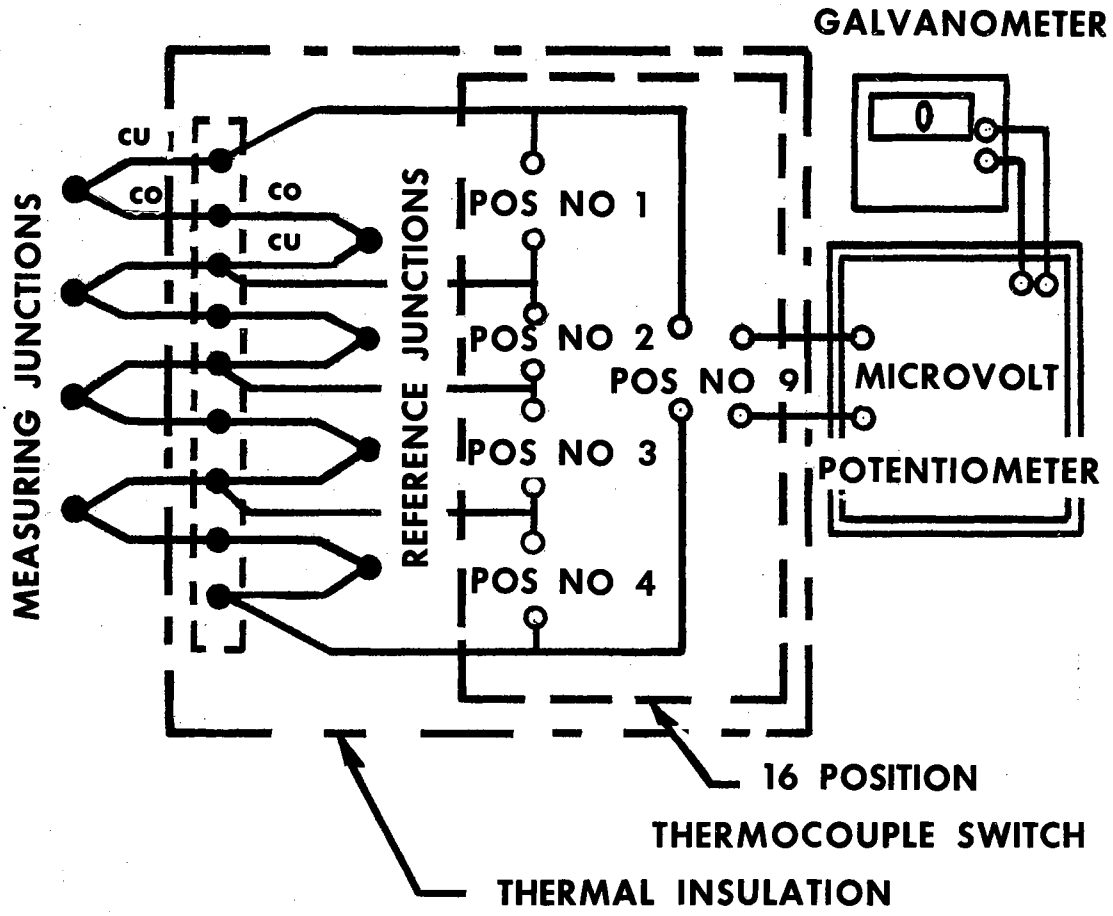

FIGURE 8- THERMOCOUPLE CIRCUIT FOR THE MEASUREMENT OF HOT PLATE BOTTOM TEMPERATURE (HPBT)

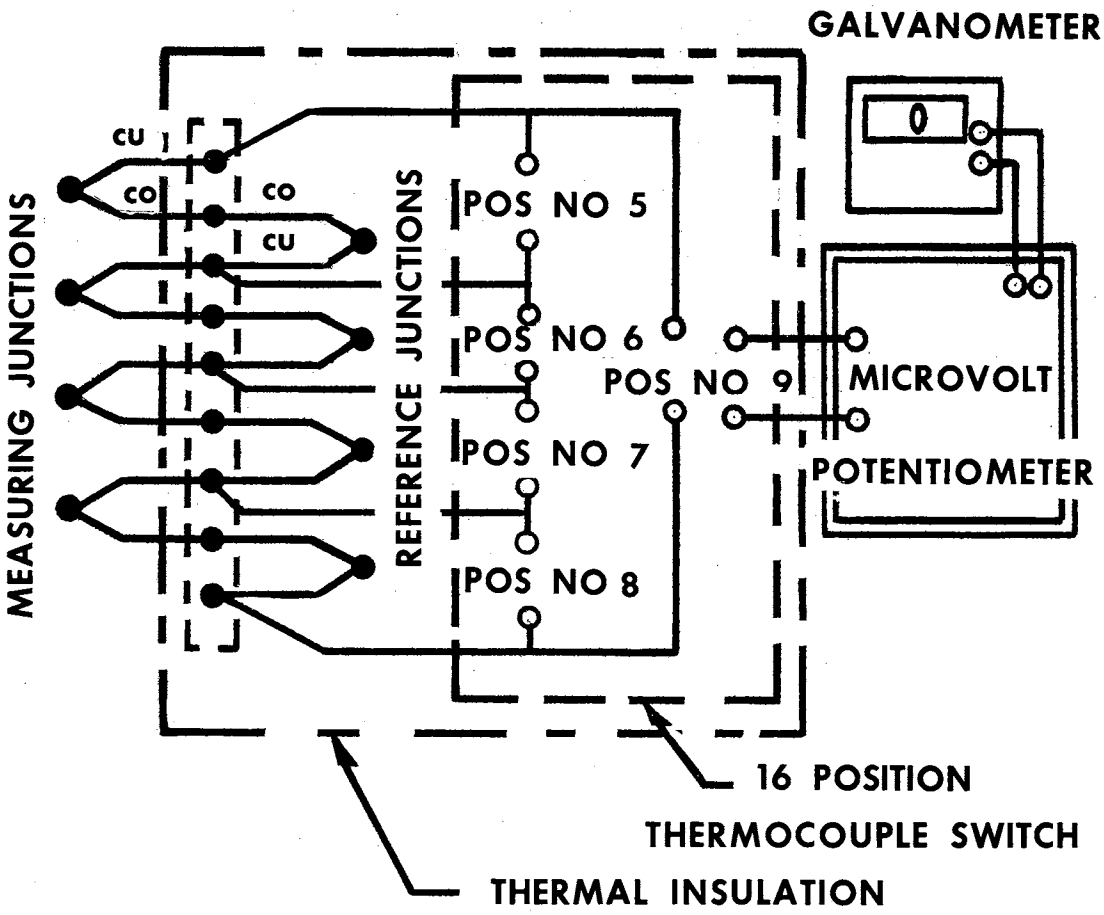

FIGURE 9- THERMOCOUPLE CIRCUIT FOR THE MEASUREMENT OF COLD PLATE TEMPERATURE(CPLT)

metals. Another distinct advantage is that only copper lead wires were used and again only copper-to-copper connections were used. In each case, the thermocouples were arranged to permit reading of individual thermocouples as well as the sum of the four thermocouples. The individual readings indicated temperature gradients that may exist across the surface. In the case of the quadruple reading, the arithmetic average was determined by the computer program and the temperature calculated using the emf-millivolt equation determined during the calibration phase.

In the case of the Hot Plate Top Temperature (HPTT) and the Top Plate Guard Temperature (TPGT), a minimum differential was desired. Therefore, a strip chart recorder was used to display the respective sums as shown in Figure 10. If the two pens indicate a disparity in temperature, the Top Plate Guard Temperature could be adjusted to decrease the temperature differential to less than one degree. A similar arrangement was used to compare Hot Plate Guard Temperature (HPGT) with the average temperature of the heater element, as shown in Figure 11. The 2:1 voltage divider divides the arithmetic average of eight thermocouples by two before comparison with the four thermocouple output of the Hot Plate Guard Temperature (HPGT).

Instrumentation

The test apparatus, vibration equipment, thermocouple network, heater measurement circuit and D.C. power supplies were arranged as shown in Figure 12. The test apparatus was rigidly bolted to the shake table of the vibration machine, and the water temperature control system attached.

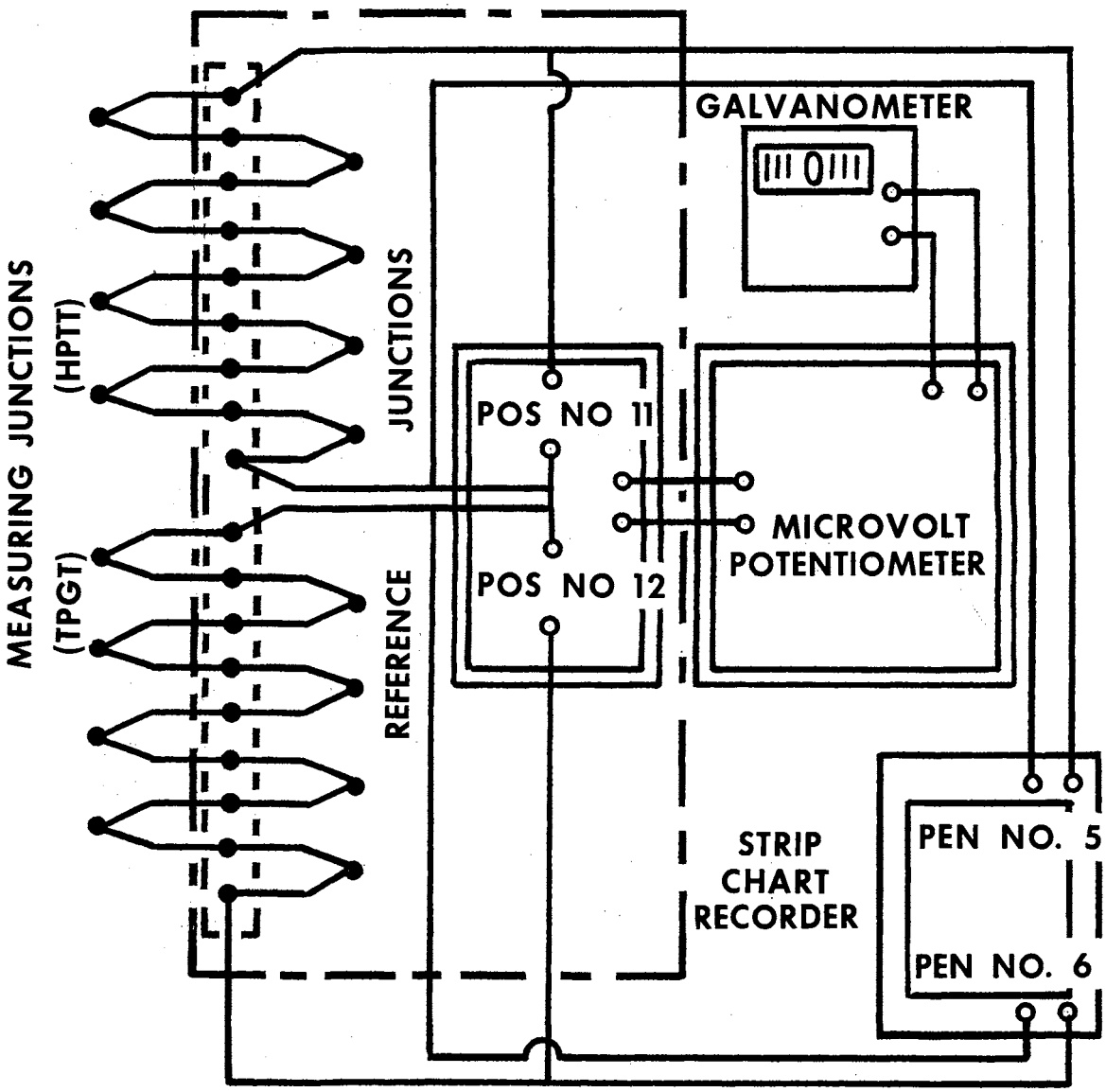

FIGURE 10- CIRCUIT FOR THE MEASUREMENT OF TOP PLATE GUARD TEMPERATURE (TPGT) AND HOT PLATE TOP TEMPERATURE(HPTT)

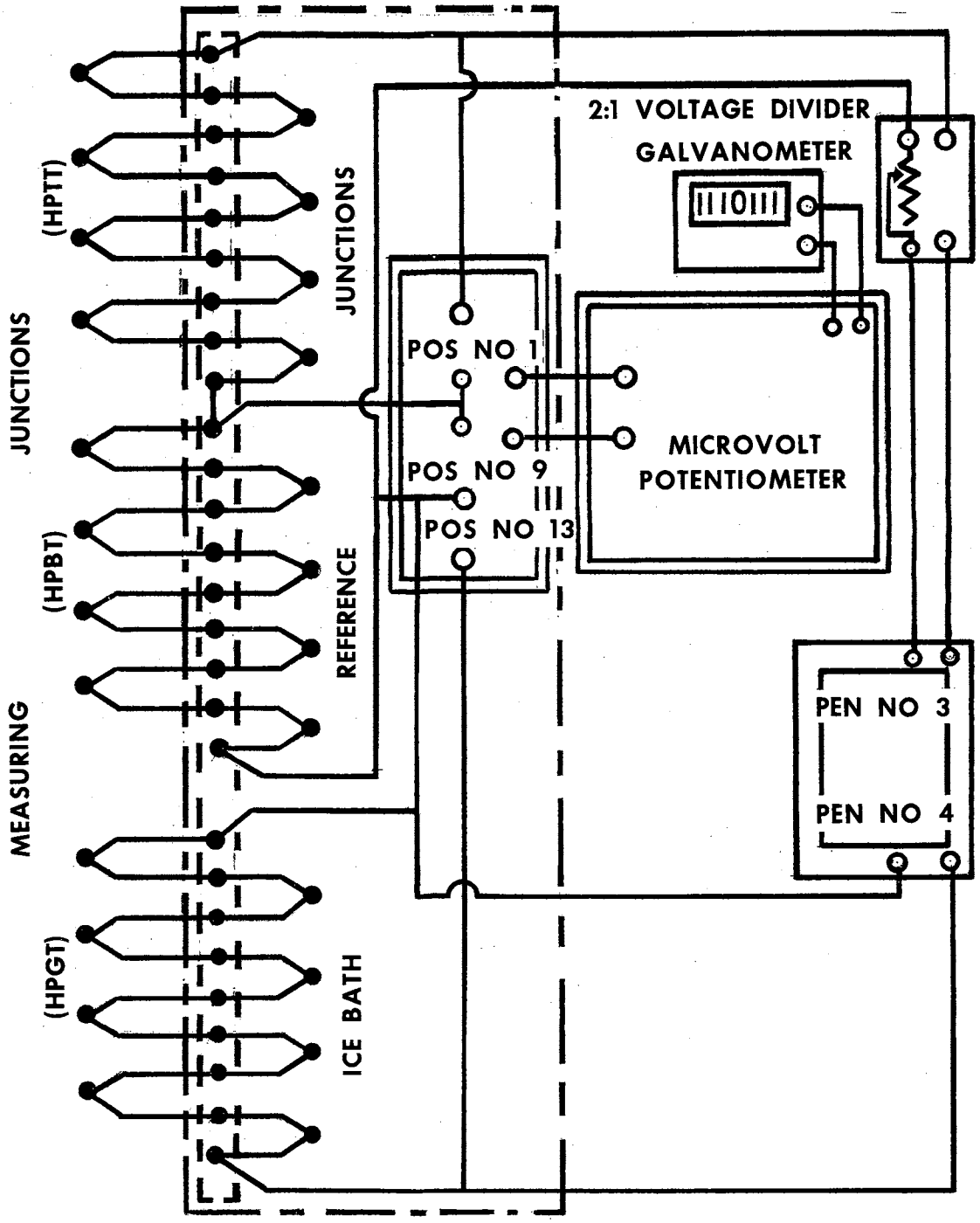

FIGURE 11- CIRCUIT FOR THE MEASUREMENT OF HOT PLATE TOP TEMPERATURE (HPTT), HOT PLATE BOTTOM TEMPERATURE (HPBT), AND HOT PLATE GUARD TEMPERATURE (HPGT)

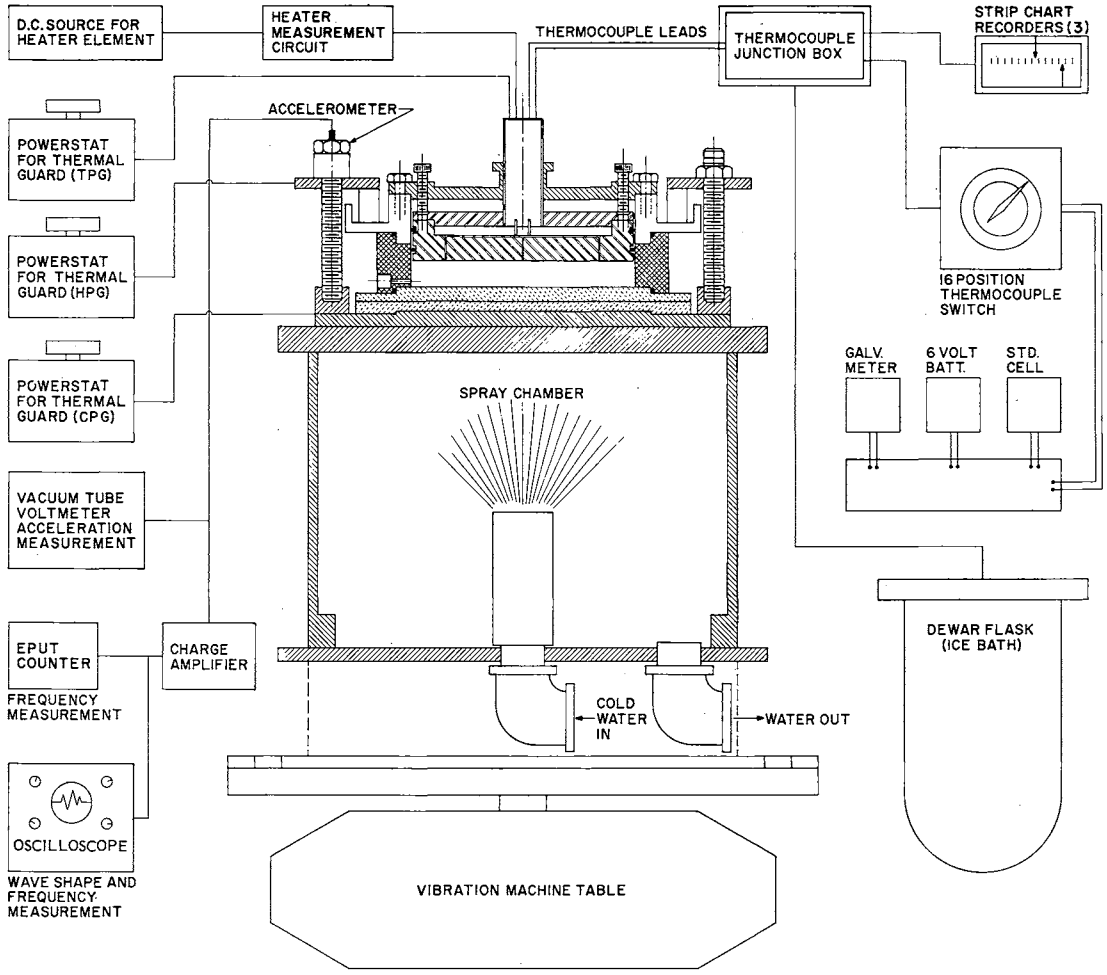

FIGURE 12- ASSEMBLY

The water temperature control system consisting of a hot water valve, a cold water valve, and a mixing valve, provided a means of varying the temperature of the cooling water from a minimum of 60°F to a maximum of 180°F. Water temperature control is necessary to control the temperature gradient across the liquid sample, and to control the average bulk temperature within close tolerances since the thermal conductivity of a liquid is a function of temperature.

Regulated D.C. power supplies, with vernier controls, were used to provide power to the heater elements of the Top Plate Guard and the Hot Plate Guard. These heater elements accomplish the important function of thermal guarding to the heater element to minimize heat losses. D.C. power supplies were chosen that had voltage ripple characteristics of less than two percent to preclude generating magnetic fields along the lead wires which could cause spurious emfs in the thermocouple wires.

A Heater Measurement Circuit was designed to accurately measure the electrical power to the heater element. The circuit and component accuracy is shown in Figure 13 and is described in detail in Chapter III.

Particular attention was directed toward the selection of a potentiometer and galvanometer that would afford maximum accuracy in reading the emf output of the thermocouples. The potentiometer chosen was a six-dial instrument with a low range of 0 to 11,111.1 microvolts in steps of 0.01 microvolts. The principle design feature of this potentiometer in addition to 0.01 microvolt sensitivity was its freedom from adventitious emfs of thermal origin. To this end, all sliding contacts were excluded from the measuring circuit which contains only manganin

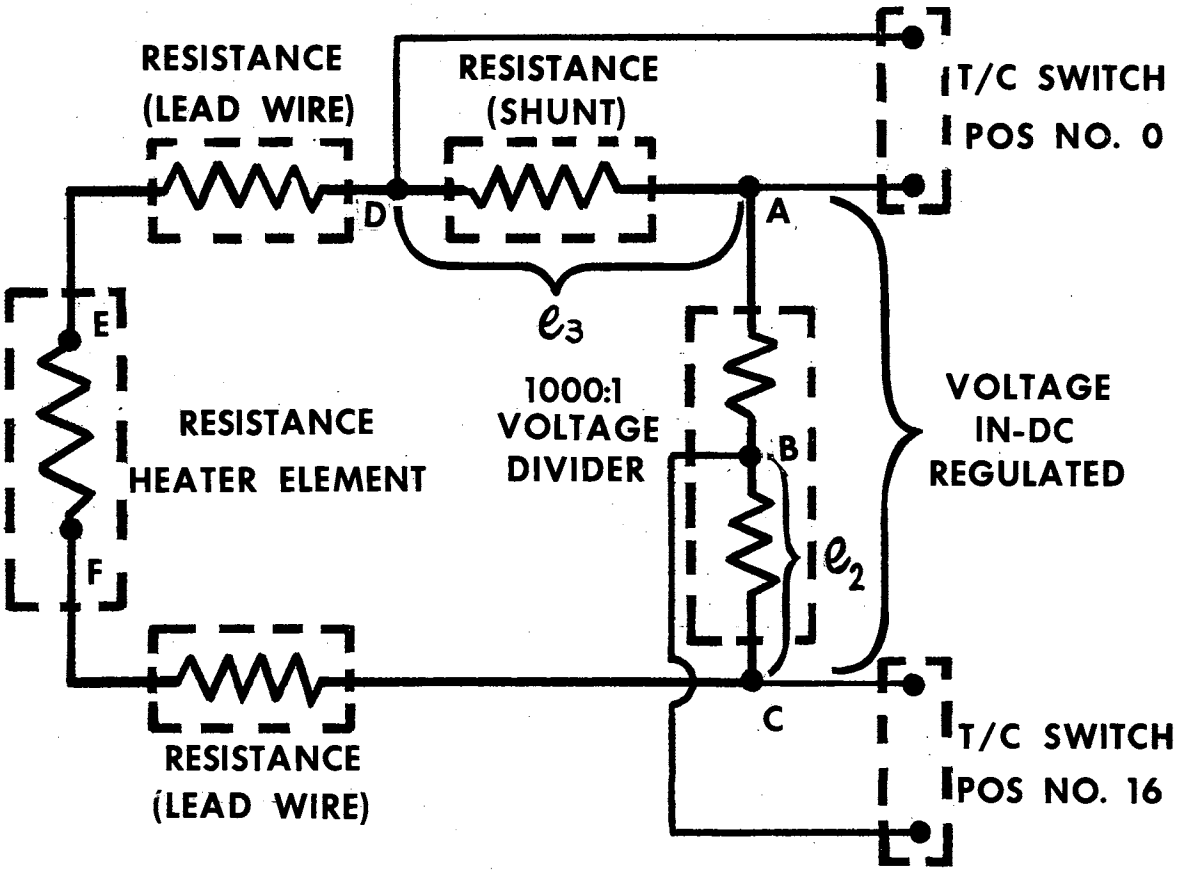

COMPONENT	AMPERES VS. RESISTANCE CALIBRATION			
	1.0 AMP.	2.0 AMP.	3.0 AMP.	ACCURACY
VOLTAGE DIVIDER (RATIO)	1004.7:1	1003.1:1	999.985:1	±0.01%
PRECISION SHUNT RESISTANCE (OHMS)	0.010021	0.010021	0.010028	±0.000010
LEAD WIRE RESISTANCE (OHMS)	0.010090	0.010102	0.010090	±0.000010

FIGURE 13- SCHEMATIC FOR MEASUREMENT OF HEAT SUPPLIED (QIN)

resistors. The potentiometer was especially designed to provide thermal symmetry which assures uniform temperatures at all vulnerable points. Although the potentiometer is essentially free from parasitic thermal emfs, any galvanometer used in conjunction with this instrument may contain a thermal emf of significant magnitude at the low thermocouple signal level. However, a galvanometer reversing key, located within the thermal shield of the potentiometer, renders the measurement independent of any galvanometer thermal emfs. In addition to nullifying thermal emfs, the use of this reversing key effectively doubles the galvanometer sensitivity. A galvanometer was selected which required an external resistance for critical damping which was slightly less than the sum of the resistance of the potentiometer and the thermocouple circuit. The sensitivity of the galvanometer was sufficient to give a perceptible deflection for one step of the last dial used. The potentiometer selected as a six-dial Thermofree Potentiometer Model 2768, manufactured by Honeywell, Incorporated. The galvanometer chosen was a Model 2430-C manufactured by Leeds-Northrup Company.

The instrumentation was assembled and located in a copper screened room. The screened copper walls afforded a minimum variation in atmospheric temperature and minimized the influence of magnetic disturbances upon the delicate, sensitive instrumentation. Figure 14 shows the instrumentation assembled inside the screen room and Figure 15 shows the arrangement of instrumentation and associated equipment outside the screen room.

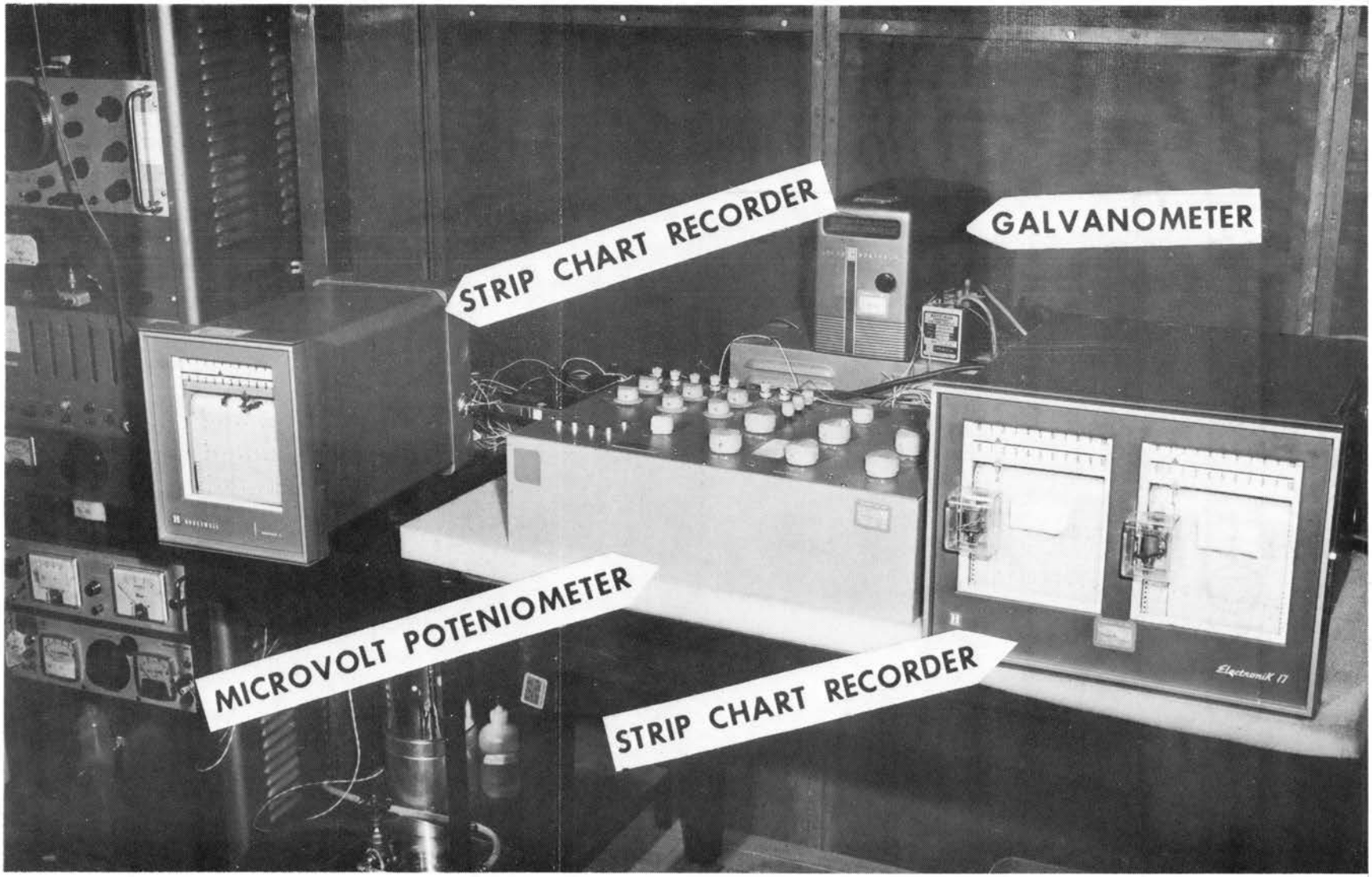

FIGURE 14- INSTRUMENTATION INSIDE SCREEN ROOM

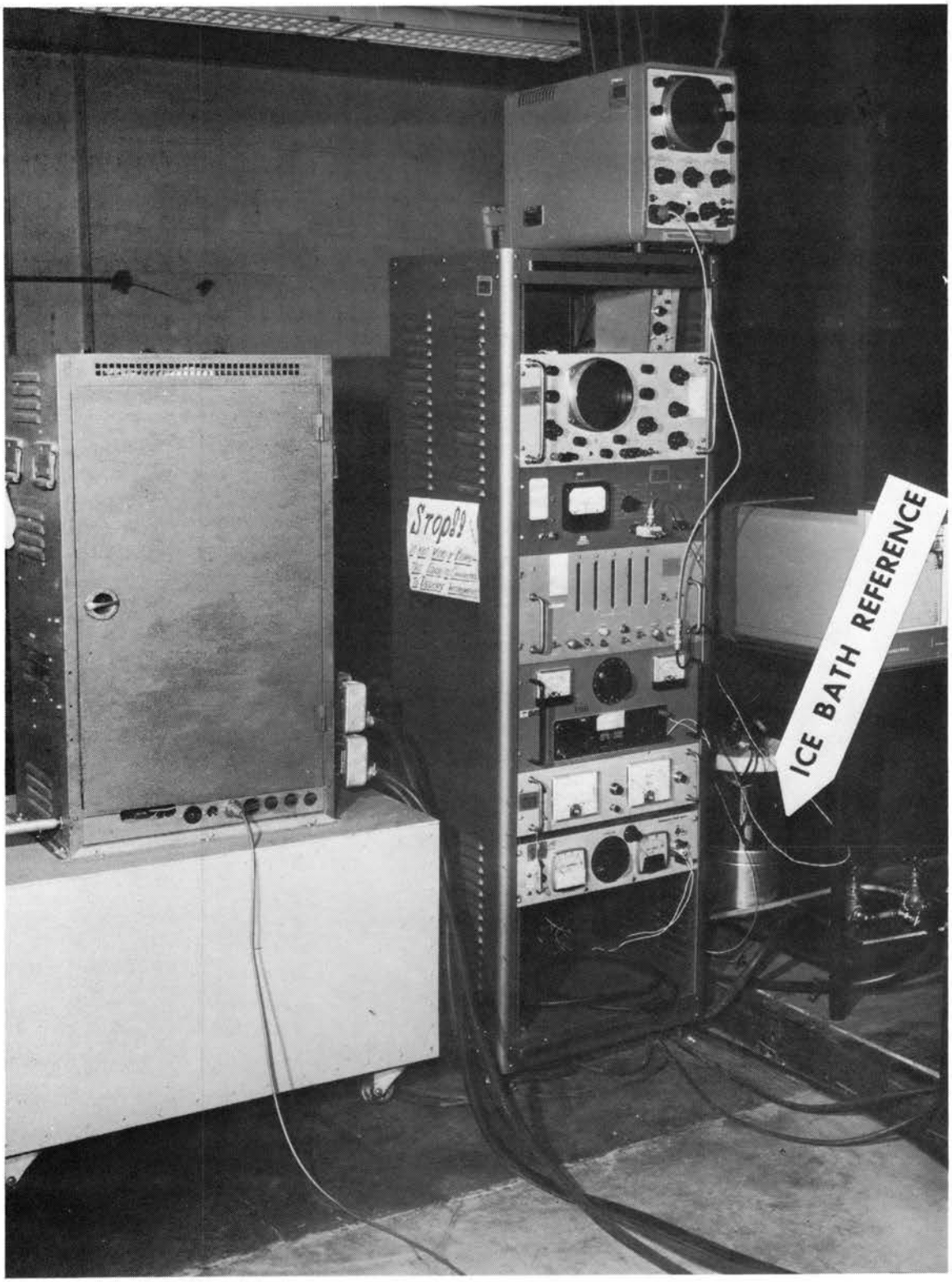

FIGURE 15- INSTRUMENTATION OUTSIDE SCREEN ROOM

CHAPTER III

DETERMINATION OF THERMAL CONDUCTIVITY

Introduction

The calculation of thermal conductivity of a liquid is predicated upon the accurate measurement of the quantity of heat transferred through the medium. With reference to Figure 16, the quantity of heat transferred through the liquid medium was designated as Q (corrected). The original amount of heat applied to the heater element was designated as Q(IN) and all possible heat exchanges with the surroundings were arranged in numerical order and numbered Q_1 through Q_{11}. Q(L) represents the total heat gain (or loss), or

$$Q(L) = Q_1 + Q_2 + \ldots\ldots Q_{11}, \text{ then}$$

$$Q(COR) = Q \text{ (corrected)} = Q(IN) + Q(L)$$

Once the value of Q(COR) is determined, the basic equation for thermal conductivity can be used to calculate the value for thermal conductivity of a liquid. Or,

$$K = Q(COR)\ (\Delta X)/(A)\ (\Delta T)$$

Where ΔX represents the linear separation of the two heat transfer surfaces, A represents the total area and ΔT represents the difference in temperature across the liquid sample. This chapter discusses the procedure for calculation of Q(IN), Q(L), Q(COR), and K_L. An

electric circuit analogy introduces alternate comparable resistance terms R_O and R_p, which provides an alternate approach.

Calculation of Q(IN)

Two methods are commonly used among investigators for determining the amount of heat supplied to the heater element, the calorimetric method and the electrical method. The calorimetric method involves measuring the temperature increase in a stream of water flowing against the cold plate. An electrical method was developed and used in this experiment simply because it afforded a means of measuring Q(IN) more accurately than any other method could provide. This method was accomplished by the use of components arranged in the schematic as shown in Figure 13. The most accurate measurements of electrical quantities using available laboratory equipment is potential (millivolts), resistance (ohms), and a voltage divider (ratio out to ratio in). The potentiometer, described earlier was readable to 0.01 microvolts, using a high-sensitivity galvanometer to detect a null balance. The resistance of the 50 milliampere shunt and the lead wire resistance are accurate to within $\pm$0.00001 ohms. To further enhance the over-all accuracy, the resistance of the lead wires, shunt and the voltage divider were calibrated as a function of amperes of current in the heater circuit and computer programmed to provide for the associated change. Although current cannot be determined accurately as a result of a direct reading, it can be determined accurately indirectly. This is accomplished by measuring the potential over a small, very accurately known, resistance. This explains the presence of the precision shunt in the circuit.

The voltage divider, constructed solely of manganin resistors, divided the input voltage in the ratio of 1000:1. This reduced the potential across the points B to C to millivolts, and readable with a microvolt potentiometer. The potential difference across the points B to C, multiplied by the voltage divider ratio, yielded the potential difference between points A and C. The measurement of the potential across the shunt provided an accurate determination of the current through the heater loop using the relationship

$$i_h \text{ (heater loop)} = \frac{e \text{ (potential across shunt)}}{R \text{ (resistance of shunt)}} .$$

The voltage e_h, across the heater element was determined by subtracting the voltage drop across the shunt and the lead wire resistance, from the voltage A to C.

Hence,

$$e_h\text{(heater)} = e \text{ (A to C)} - i\ (R_{ST} + R_{LT}).$$

The value of Q(IN) is simply the product of $e_h i_h$.

In summary, the procedure for the measurement of Q(IN) (BTU) was as follows:

a. Read e_2.

b. $e_1 = (e_2)$ (VDR),

where VDR is the voltage divider ratio and is given by the following current dependent relationship VDR = 1006.3 - 1.6 (i_h). i_h is the current through heater element and was assumed zero for the first computer iteration.

c. Read e_3.

d. $i_h = e_3/R$ (resistance of shunt)

e. $e_h = e_1 - i_h\ (R_{LT} + R_{ST})$.

Where R_{LT} is the temperature dependent resistance value of the leads and is expressed as a function of amperes as

$$R_{LT} = 0.03890 = i_h\ (0.00012).$$

R_{ST} is the temperature dependent resistance value of the shunt and is expressed as a function of amperes as

$$R_{ST} = 0.01002109 + i_h\ (0.00000013).$$

f. Q(IN) (watts) = $i_h e_h$.

g. Q(IN) (BTU/hr) = Q(IN) (watts) x 3.41520.

It is important to note that this method permitted compensation for the change of resistance due to heating attributed to current flow. With computer programming, the correct i_h was calculated, as in step d, then the i_h was used to calculate the correct values of all resistances in the circuit. It should also be noted that this method does not depend upon knowing the value of the resistance in the heater which also varies with temperatures.

Calculation of Q(L) (Heat Loss)

In Figure 16, the cross sectional view of the test chamber, the placement of thermocouples, the physical relationship of the mating parts and the possible modes of heat transfer are shown. With reference to Figure 16, Q(L) is identified as being the sum of all heat exchanged between the heater element and the surroundings, exclusive of the heat transferred through the liquid sample to the cold plate, or

$$Q(L) = \Sigma\ (Q_1 + Q_2 + \ldots + Q_{11})$$

Q(L), the heat loss (or gain), is applied to Q(IN) by computer programming, to determine the actual value of heat transferred through

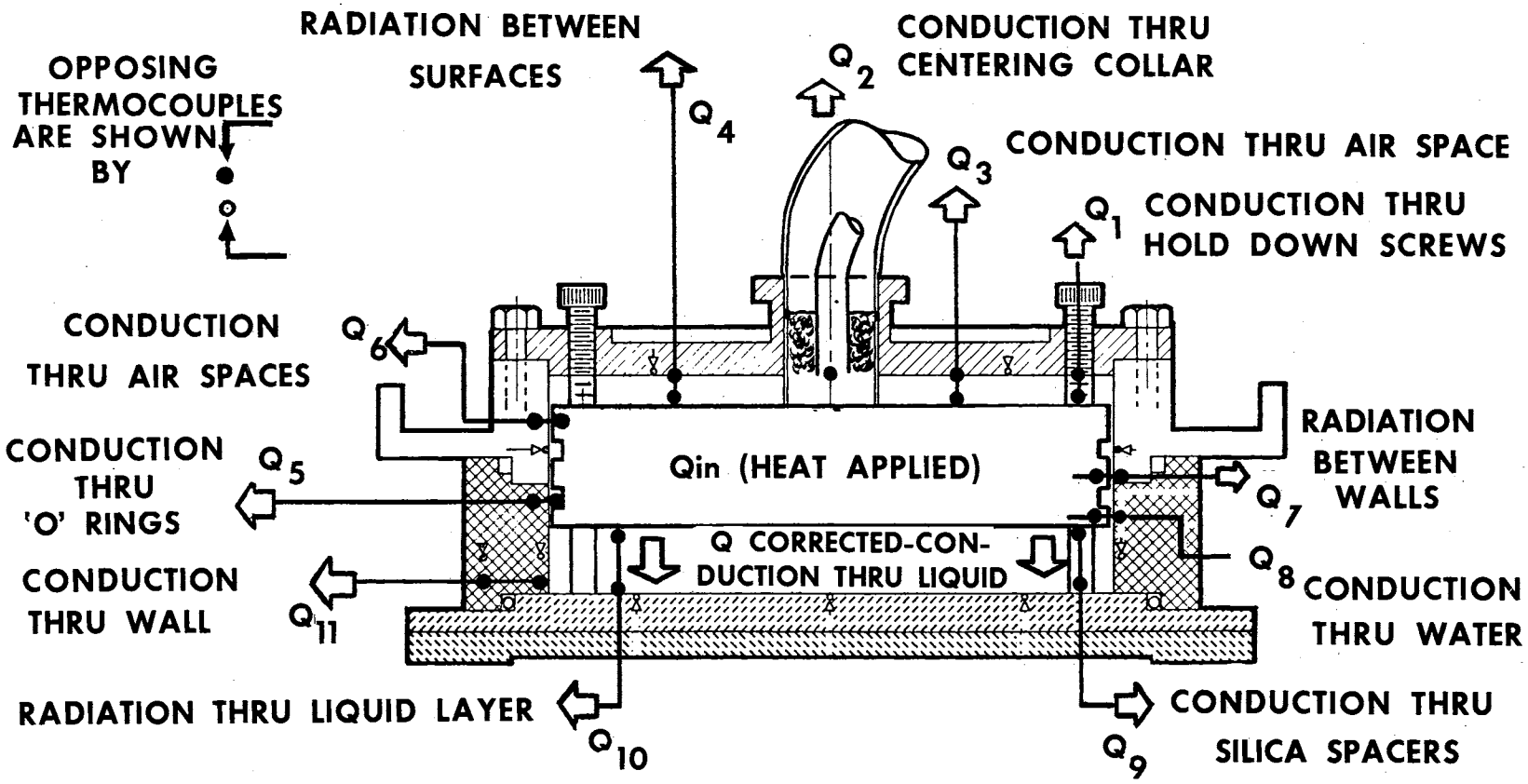

FIGURE 16— POSSIBLE MODES OF HEAT TRANSFER

the liquid sample or:

$$Q(IN) \pm Q(L) = Q(COR).$$

In the interest of clarity, the calculation of Q(L) will be discussed in the following columnar format in Table II.

Column A - Q_n--Identification as to the mode of heat transfer, where $Q_n = Q_1, \ldots Q_{11}$

Column B - Temperature differential

Column C - Linear separation of heat sources

Column D - Assumptions and basis for assumptions

Column E - Equation used to evaluate heat flow, and Q_n calculated for one degree of temperature differential to provide an understanding of the relative magnitude of the quantity of heat transferred.

TABLE II

CALCULATION OF Q(L)

A	B	C	D	E
Q_n - Mode of Heat Transfer	Temperature Differential	Linear Separation of Heat Sources	Assumptions and Basis	Equations of Heat Transfer and Evaluation for One Degree Temperature Differential
Q_1 - Heat exchange between element and Top Plate Guard, by conduction through hold down screws	HPTT - TPGT or $\Delta T(1)$	$\Delta X(1)$	None	$Q_1 = (K_{SCT})(ASC)(3)\Delta T(1)/\Delta X(1)$ $Q_1 = (7.760)(2.1815 \times 10^{-4})(3)(1°)/0.05$ $Q_1 = 0.10157$
Q_2 - Heat exchange through the thin stainless steel centering bushing	$\Delta T(1)$	$\Delta X(1)$	None	$Q_2 = (K_{SBT})(ASB)\Delta T(1)/\Delta X(1)$ Where K_{SBT} is the same value as used for screw material, ASB is cross sectional area of bushing. $Q_2 = (7.760)(5.576 \times 10^{-4})(1°)/0.05$ $Q_2 = 0.086538$

TABLE II (Continued)

A	B	C	D	E
Q_n - Mode of Heat Transfer	Temperature Differential	Linear Seperation of Heat Sources	Assumptions and Basis	Equations of Heat Transfer and Evaluation for One Degree Temperature Differential
Q_3 - Heat exchange by conduction, through the thin layer of air separating the Top Plate Guard and Hot Plate Top	$\Delta T(1)$	$\Delta X(1)$	Heat exchange by conduction only[1]	$Q_3 = K_{AT} A_p \Delta T(1)/\Delta X(1)$ Where K_{AT} represents the temperature dependent thermal conductivity of air at the mean temperature $K_{AT} = 0.0133+(0.000021)(HPTT+TPGT)/2$ Ap is the area of the horizontal circular plate $Q_3 = (0.0133)(0.095618)(1°)/0.05$ $Q_3 = 0.025424$
Q_4 - Heat exchange by radiation between Hot Plate Top and	$\Delta T(1)$	$\Delta X(1)$	The surfaces are assumed gray, separated by a nonabsorbing medium, with a	$Q_4 = A_1 F_{12} \sigma[(TPGT+460.0)^4-(HPTT+460.0)^4]$ Where $A_1F_{12}=P_1/A_1E_1+1/A_1+P_2/A_2E_2=0.0152436$ $\rho_1=\rho_2$ (reflectivity of Hot Plate Top and

[1] W. O. Carlson, Ph.D. Thesis, University of Minnesota, Minneapolis 1952

TABLE II (Continued)

A	B	C	D	E
Q_n - Mode of Heat Transfer	Temperature Differential	Linear Separation of Heat Sources	Assumptions and Basis	Equations of Heat Transfer and Evaluation for One Degree Temperature Differential
Q_4 (Continued) Top Plate Guard			view factor of unity. Gray surfaces are assumed since the copper surfaces cleaned and polished have a constant emissivity of 0.035 for the average operating temperature ± 100°F.	Top Plate Guard respectively) = 0.965 $A_1 = A_2$ area of surfaces = Ap $E_1 = E_2$ (emittance of surface) = 0.035 If TPGT is assumed to be 140°F, HPTT is assumed to be 141°F, $Q_4 = (0.0152436)(0.1714x10^{-8})(600)^4-(601)^4$ $= (0.24121)(18.65)$ $Q_4 = -0.048715$
Q_5 Heat exchange conduction through the two "O" ring seals separating the heater element and the Hot Plate Guard	$\Delta T(3)$ where $\Delta T(3) = (HPTT + HPBT)/2 - HPGT$	0.020"	None	$Q_5 = K_{OR}(2\pi L)(T_i-T_o)/\ln(r_o/r_i)$ Where K_{OR} is the thermal conductivity of "O" ring material (0.0873), L is vertical distance of contact of the "O" ring seal (0.045"), r_o is outside radius of "O" ring and r_i is inside radius of "O" ring. $Q_5 = (0.087)(2.4518)(1°)$

TABLE II (Continued)

A	B	C	D	E
Q_n - Mode of Heat Transfer	Temperature Differential	Linear Separation of Heat Sources	Assumptions and Basis	Equations of Heat Transfer and Evaluation for One Degree Temperature Differential
Q_5 (Continued)				$Q_5 = 0.21518$
Q_6 - Heat exchange through the air layer separating the vertical cylindrical surfaces of the heater element and the Hot Plate Guard	$\Delta T(3)$	0.020"	It is assumed heat exchange is by conduction only. When a fluid layer is enclosed between two vertical surfaces and the associated Grashof number is less than the value $12^4(Pr)^{-2}(20/21+Pr)(1/b)$ where L equals the height of the layer and be equals the thickness, the temperature decreases linearly in the fluid layer in a direction normal	$Q_6 = (K_{AT})(2\pi L_1)\, T(3)/\ln(r_o/r_i)$ Where K_{AT} = thermal conductivity of dry air, temperature dependent as calculated earlier. L is the vertical dimension of the wall between the heater element and the surrounding wall. If $\Delta T(3)=1°$, $Q_6 = (0.0133)(14.1000)(1°)$ $Q_6 = 1.8795$

TABLE II (Continued)

A	B	C	D	E
Q_n - Mode of Heat Transfer	Temperature Differential	Linear Separation of Heat Sources	Assumptions and Basis	Equations of Heat Transfer and Evaluation for One Degree Temperature Differential
Q_6 (Continued)			to the two walls, over the major portion of the layer. In this case the above term, when evaluated at 200°F, equals $124(0.72)^{-2}(20/21+0.72)9.900/0.002=124(1.930)(1.670)(450)=180,000$ whereas the Grashof number is 4,919, therefore, conduction only is assumed.	
Q_7 - Heat exchange by radiation between the	$\Delta T(3)$	.002"	Gray surfaces, with a nonabsorbing medium is assumed since	$Q_7 = A_3 F_{34} \sigma (T_3^4 - T_4^4)$ Where T_3 = average temperature of the heater element (HPTT+HPBT)/2 in degrees

TABLE II (Continued)

A	B	C	D	E
Q_n - Mode of Heat Transfer	Temperature Differential	Linear Separation of Heat Sources	Assumptions and Basis	Equations of Heat Transfer and Evaluation for One Degree Temperature Differential
Q_7 (Continued) vertical, cylindrical surfaces of the heater element and the Hot Plate Guard			the emittance of the polished chromium surfaces at operating temperature is 0.030 and the emittance for the polished aluminum surface of the Hot Plate Guard is 0.100 The shape factor is considered unity (1.0) since the diametrical clearance is only 0.020.	Rankin T_4 = temperature of Hot Plate Guard (HPGT) in degrees Rankin $A_3F_{34}=1/P_3+1=P_4/A_3E_3A_3A_4E_4=0.0194\,2007$ and subscript 3 indicates properties pertaining to surface of heater element and subscript 4 indicates properties of surface of Hot Plate Guard. If Hot Plate Guard is (141°F), (601°R) heater element is (140°F), (600°R) substituting values in above equation. $Q_7 = (0.1713\times10^{-8})(0.1942007)(601)^4$ $= (600)^4$ $Q_7 = (0.0033266)(18.65) = 0.0620$

TABLE II (Continued)

A	B	C	D	E
Q_n - Mode of Heat Transfer	Temperature Differential	Linear Separation of Heat Sources	Assumptions and Basis	Equations of Heat Transfer and Evaluation for One Degree Temperature Differential
Q_8 - Heat exchange through the thin cylindrical layer of water between the bottom "O" ring and the bottom of the heater	$\Delta T(4)$ $\Delta T(4)$ is calculated by a computer program (relaxation techniques) using boundary conditions of HPGT, HPBT and CPLT.	0.020"	None	$Q_8 = CPL\ (2\pi L_3)\Delta T(^4)/\ln(r_o/r_i)$ Where CPL is the thermal conductivity of the plastic test chamber $Q_8 = (0.12)\ (0.0044)\ (\Delta T(4))$ $Q_8 = (0.12)\ (0.0044)(1^9) = 0.000528$ L_3 is the vertical dimension of the thin cylindrical water layer.
Q_9 - Heat exchange by conduction through the fused silica spacers, between the bottom of the heater element and the Cold Plate	$\Delta T(2)$	$\Delta X(2)$	None	$Q_9 = 3K_{QT})(A)\Delta T(2)/\Delta X(2)$ K_{QT} is the thermal conductivity of fused silica (K=0.45). Normally $\Delta T(2)$ equals approximately 10°F letting $\Delta T(2)$=10°F and $\Delta X(2)$ = 0.300". $Q_9 = 3(K_{\Delta T})(AFS)(10/0.300")/12=3(0.45)(2.1815)(10^{-4})(10^{o})(120)/0.300$ $Q_9 = 0.11780$

TABLE II (Continued)

A	B	C	D	E
Q_n - Mode of Heat Transfer	Temperature Differential	Linear Separation of Heat Sources	Assumptions and Basis	Equations of Heat Transfer and Evaluation for One Degree Temperature Differential
Q_{10} - Heat exchange by radiation through the liquid sample, between the bottom of the heater element and the Cold Plate	$\Delta T(2)$	$\Delta X(2)$	Parallel, gray, diffuse surfaces	$Q_{10}=(A_5F_{56})(e_1e_2/1-\rho_1\rho_2)\sigma\tau(HPBT+460)^4 -(CPLT+460)^4$ Where A_5 is the surface area of Hot Plate F_{56} is the shape factor between the surfaces; e_1 and e_2 is the emissivity of the surfaces (0.10); ρ_1 and ρ_2 is the reflectivity of the surfaces (0.90), τ is the transmissivity of the liquid. $Q_{10}=(0.0956183)(5.263x10^{-4})(0.1714x10^{-8})(\tau)[(5.70)^4-(5.50)^4]$ $Q_{10} = 0.00121215$
Q_{11} - Heat exchange through the plastic walls of the test chamber by conduction in	The heat loss in the radial direction is determined from temperature gradient in the chamber	The temperature near the inner wall (t_i) is determined by thermocouples at a radius of 2.118 inches.	None	$Q_{11} = (-K_{PL})(2\pi L)(T_i-T_o)/\ln(r_o/r_i)$ Where K_{PL} is the thermal conductivity of the plastic material, which is 0.120, L is the length of the plastic cylinder containing the liquid sample and equals $\Delta X(2)$.

TABLE II (Continued)

A	B	C	D	E
Q_n - Mode of Heat Transfer	Temperature Differential	Linear Separation of Heat Sources	Assumptions and Basis	Equations of Heat Transfer and Evaluation for One Degree Temperature Differential
Q_{11} (Continued) the radial direction	walls. The temperature gradient is detected by thermocouples embedded in the walls as shown in Figure 16. This temperature gradient is identified as $\Delta T(5)$.	The temperature near the outer wall (t_o) is detected by thermocouples at a radius of 2.500 inches. The difference in radius appears as the logarithmic function of the ration (r_o/r_i).		Q_{11} evaluated at a temperature difference of one degree ($T_i - T_o = 1°F$) assuming $\Delta X(2)$, the liquid sample thickness is 0.30". $Q_{11} = (0.120)(2\pi x 0.300/12)(1°)/\ln(2.500/2.118) = 0.0018848/0.0721$ $Q_{11} = 0.002614$ The algebraic sum of the Q_ns calculated above Q_1 through Q_{11}) represents the total heat loss (or gain) and is identified as Q(L). The signed value Q(L) is applied to Q(IN) to determine the correct value for heat flow downward through the liquid sample, or $Q(IN) + Q(L) = Q(COR)$

Calculation of R_0, R_T, and K_L

In measuring the thermal conductivity of a thin liquid layer, the following assumptions are made.

a. The mating surfaces are perfectly clean and perfectly flat without any irregularities.

b. There is no resistance due to the metal-liquid interface.

c. The thermocouples embedded on the mating surfaces detect the exact temperature of the liquid at the metal-liquid interface.

d. No instrumentation errors.

In actual practice, all these conditions are very difficult if not impossible to meet. For example, even if the metal surfaces are accurately planed, plated, polished, and lapped flat, surface irregularities of the order of 0.0005 inches are not uncommon. Additional resistance may also be introduced by a thin film of oxidized material partially coating the mating surfaces. It must also be assumed the thermocouple junction is precisely located at the liquid-metal interface, and no instrumentation errors are present in the temperature measurement. This would be very difficult to accomplish in an arrangement where the thermocouple wires must vibrate in an electromagnetic field. The thermocouple wires must cross or cut the magnetic lines of flux twice during each cycle. Therefore, during each half cycle, an emf may be generated and current flows through the thermocouple wires. However, during the remaining half of the cycle, the current is reversed and the emf reverses in sign. Although the average value is zero, we must assume that no rectification or direct

current has been generated which would be manifested as an erroneous emf to the potentiometer.

Upon examination of the basic equation to determine thermal conductivity, namely

$$K = Q\ \Delta X/A\ \Delta T$$

a comparable resistance term can be identified. From an analagous electrical circuit, the resistance term can be written

$$R_0 = \Delta T/Q = \Delta X/K_L A$$

Therefore, it would seem proper to determine the magnitude of a residual resistance which may exist due to the presence of the four factors mentioned earlier. This residual resistance can be determined by measuring the value of heat flow Q(COR) with zero separation of the Hot Plate and Cold Plate surfaces. This value of residual resistance will be identified as R_0. If a similar equation is used to express R_T, or the total resistance, the correct value of K_L can be expressed as

$$K_L = \Delta X/(R_T - R_0)A$$

The value of R_0 represents residual resistances which may originate from several sources. Therefore, R_0 was determined as a function of temperature and frequency of vibration.

Maximum Uncertainty

After the design of the test apparatus and the methodology of processing the data was completed, the writer was motivated to determine the accuracy of the data. Therefore, a mathematical model that would embrace both the design characteristics and the data

processing was conceived. The mathematical model was specifically brought into being to answer the following question:

> The values of measured thermal conductivity will have a theoretical accuracy within what limits; or, restated, what will be the "maximum uncertainty" of the final results?

With reference to Appendix D, each measured parameter, which influences the calculation of thermal conductivity, is given in Column 1, the symbol used throughout the text is given in Column 2, and the accuracy within which the measurement is known to exist is given in Column 3. In addition, the method of measurement, or the standard against which the measurement was made, is given in Column 4 and the standard or basis of calibration is given in Column 5. The equation for calculation of Q_1 from the preceding section is

$$Q_1 = (K_{SCT})(A_{SC}) \quad (3)\ \Delta T(2)/\Delta X(1).$$

Where K_{SCT} is the temperature dependent value of thermal conductivity of the three stainless steel screws, the value of which is known to be accurate within ± 0.01. A_{SC} is the cross sectional area of each screw. The diameter measurement is within micrometer accuracy of ± 0.0005 inches. $\Delta T(1)$ in this case is TPGT minus MPTT and each are accurate within $\pm 0.063^{\circ}F$ as determined earlier by the thermocouple calibration. $\Delta X(1)$ is the linear separation between the top of the Hot Plate and the Top Plate Guard and has an associated accuracy of ± 0.020 inches. If the differential of the equation is taken and the values of error are substituted for dA_{SC}

$d\Delta T(1)$, dK_{SCT} and $d\Delta X(1)$ the corresponding value of error for dQ_1 can be determined. In like manner, the error in Q_2 through Q_{11} can be found. Also, the error for Q(IN) can be determined by taking a differential of the equation

$$Qin = (e_3/R_{ST})((e_2 \cdot VDR)-(e_3/R_{ST})(R_{LP}+R_{ST})).$$

also $Q(L) \pm(error) = \Sigma(Q_1(\pm dQ_1) + Q_2(\pm dQ_2)---dQ_{11}(\pm dQ_{11}))$

then

$$Q(COR)(\pm dQ(COR)) = Qin(\pm dQin) + Q_L(\pm dQ_L)$$

The value of K_L is given by

$$K_L = Q(COR)\ \Delta X/A\ \Delta T(1)$$

Taking a differential and evaluating dK_L by inserting values for dQ(COR) $d\Delta X$, dA and $d\Delta T$, yields a value for the error or uncertainty of K_L. However, it must be observed this is not the maximum value of deviation or uncertainty. An upper bound is obtained if all positive error values are substituted in the numerator and all negative values are substituted in the denominator, and lower bound is obtained by the reverse order. The upper bound or limit minus the lower bound yields the maximum uncertainty in the measurement of K_L.

With this uncertainty known, as a function of each parameter measured, a valuable analytical tool in the form of a computer program was brought into being. Its purpose was not only to calculate maximum uncertainty, but to serve as a tool which can be used to identify and improve methods of measurement which contribute most significantly to the magnitude of the uncertainty. With this

mathematical model in existence as a computer program, the test procedures as outlined in Chapter IV resulted in the test data of Chapter V, and the conclusions of Chapter VI.

CHAPTER IV

METHOD AND PROCEDURE

Test Procedure

Preparation for the recording of data and subsequent calculation of thermal conductivity consisted of the following:

a. Preparation of Dewar Flask - The ice bath reference was prepared in strict accordance as outlined earlier during the calibration. Distilled water was frozen and chipped into "pea-sized" pieces and placed in the flask. Distilled water was added to fill the interstices and to approximately three inches of the top. The thermocouples immersed in kerosene were placed in the ice bath. Approximately six hours elapsed before readings were taken to insure thermal equilibrium had been reached.

b. Instrumentation Check - All instruments werecarefully zeroed or checked for proper reference. Careful attention was directed particularly to the zeroing of the standard cells of the microvolt potentiometer.

Prior to a test run for each film thickness, the test chamber was assembled using the appropriate spacers. Before assembly, the individual pieces were washed in a mild detergent, sterilized in hot distilled water, rinsed, and dried with an inert gas. The chamber was carefully assembled, spacers inserted, and the heater element

lowered into place. The Top Plate Guard was screwed down and the hollow hold down screws advanced against the top of the heater element until the heater element was firmly against the flat surfaces of the fused silica spacers. Electrical power was applied to the heater element and the surrounding guard heater. Distilled water was boiled for purposes of deaeration; the fill stop-cock opened and the liquid test chamber slowly filled. Careful attention was given to the formation of bubbles on the highly polished surfaces of the test chamber. A bright light entering from the opposite side from the observer made the presence of bubbles easy to detect. A slight tilting of the chamber would permit the bubbles to escape. When the chamber was filled with no bubbles present, the vent hold was closed, the fill stop-cock closed, and the chamber leveled.

The thermocouple probes of the Hot Plate Guard and Temperature Inside (TI) and Temperature Outside (TO) were inserted. The water control valves were adjusted in conjunction with the rheostat for electrical power to the heater element to provide a constant average bulk temperature of 93°F. The strip chart recorders were carefully monitored for temperature equilibrium between heater element and guard heaters. A minimum of twenty minutes was allowed after thermal equilibrium was reached before readings were taken. The first three recordings were used to determine thermal conductivity under static conditions. After each recording, the test chamber was again visually inspected to detect possible bubble formation before proceeding. After three runs under static conditions, the motor-generator set was energized, the frequency was set using the EPUT meter and

the amplitude adjusted for 1.0 G while monitoring the vacuum-tube voltmeter. The calibrated accelerometer used had an output of 4.0 millivolts at 1.0 G. The heater element and guard heater were again adjusted for thermal equilibrium and a bulk temperature of 93°F. As in the case of static conditions, 20 minutes of thermal equilibrium elapsed before recordings were made. The sample thicknesses were 0.10, 0.20, 0.30, 0.40, 0.50 and 0.60 inches. For each thickness, the thermal conductivity was measured for frequencies of 0, 6.5, 8.0, 10.0, 12.0, 14.0, 16.0, 18.0, 20, 40, 60, 80, 100, 200, and 300 cycles per second.

Sample Calculation

For the purpose of illustration, the observed data from run #530 was used. This run was chosen because it represents a run of average film thickness (0.500 inches) and frequency (15 CPS). During run #530, the following pertinent data was observed, recorded, and the following calculations were made by the IBM 7090 computer program listed under Appendix G.

Thermocouples	emf Reading (mv)	Temperature Computed (°F)
HPBT (4^T/C)	7.6150	116.4558
CPLT (4^T/C)	3.3055	69.9604
HPTT (4^T/C)	7.7633	118.0209
TPGT (4^T/C)	7.7870	118.2708
HPGT (4^T/C)	7.7063	117.4196
TI (4^T/C)	4.1617	79.5306
TO (4^T/C)	4.1077	79.4098

From the above temperature computation, the following differential temperatures were calculated

$\Delta T(1) = TPOT - HPTT = 118.2708° - 118.0209° = 0.2499°$

$\Delta T(3) = HPOT - (HPTT+HPBT)/2.0 = 117.4196° - 116.4558° = 0.78255°$

Following the procedure as outlined in Chapter 3, Q(IN) was calculated as follows

a. e_2 read 7.2907 mv

b. $e_1 = (e_2)$ (voltage divider ratio) = 7290.7x1003.0 = 7.312572/volts

c. e_3 read 17.9947 mv

d. $I_h = e_3/R_{ST} = 0.0179947/0.01002109 = 1.7955$ amps

e. Q(IN) (Watts) = $I_h e_h$ = 1.7955 amps x 7.23456 volts = 12.98965

f. Q(IN) (BTU/hr) = 12.98965 x 3.41520 = 44.36225

The value of Q(L), the sum of all heat losses, is determined in accordance with the procedure and equations outlined earlier.

$Q_1 = (3)(7.600)(8.864x10^{-5})(0.2499°)/0.0250) = 0.0448$

$Q_2 = (7.752)(5.5760x10^{-4})(0.2499°)/(0.0250) = 0.5372503$

$Q_3 = (0.1330)(0.095612)(0.2499°)/(0.0250) = 0.0855$

$Q_4 = (0.01524)(0.1714x10^{-8})(578.24)^4-(578.02)^4 = 0.02636$

$Q_5 = (0.0873)(6.28318)(0.050)(0.1812°)/1_n\frac{(2.1690)}{(2.1025)} = 0.0387$

$Q_6 = (0.0133)(49.0363)(-0.1812) = -0.14027$

$Q_7 = (0.01942)(0.1714x10^{-8})(579.40)^4 - 578.16)^4 = 0.061608$

$Q_8 = (0.3190)(5.4480)(0.1812°) = 0.3461764$

$Q_9 = -(3)(0.45)(1.3526 \times 10^{-4})(46.495)/(0.04169) = -0.20244$

$Q_{10} = -(0.09561)(1.00)(0.1714 \times 10^{-8})(0.1000)(576.45)^4 - (529.96)^4$

$= -0.051695$

$Q_{11} = -(0.12)(6.2831)(0.0416)/0.0721) = -0.43597$

$Q(L) = Q_1 + Q_2 + Q_3 + \ldots\ldots\ldots Q_{11} = +1.8453$

Since $Q(COR) = Q(IN) + Q(L)$

$Q(COR) = 44.36215 + 1.8453$; or

$Q(COR) = 46.2074$

$R_T = \Delta T(2)/Q(COR) = 46.4953/46.2074 = 1.1075$

R_0 was determined as 0.014518 at 15 CPS.

K_L (Thermal conductivity of the liquid) is expressed earlier as

$K_L = \Delta X(2)/(R_T - R_0)\ A$, and evaluated as

$K_L = 0.04169/(1.107514 - 0.014518)(0.095618) = 0.398908$

K_S (Thermal conductivity under static conditions), is calculated in the same manner, from results of previous run No. 501 was 0.340010.

The dimensionless Ratio K_L/K_S was 0.34440/0.34000 = 1.01294.

dK_L (maximum uncertainty) computed in accordance with procedure outlined in Chapter III was ± 0.00585877 and the error is, therefore, ± 1.700 percent (0.00585/0.34440).

CHAPTER V

TEST RESULTS AND CORRELATIONS

Experimental Data

Measurement of Residual Resistance R_0

In Chapter III a residual resistance term was identified as:

$$R_0 = \Delta T/Q = \Delta X/K_L A.$$

This residual resistance was determined by measuring the value of heat flow, Q corrected, with zero separation between the hot plate and cold plate surfaces. The values of R_0 were determined as functions of temperature and frequency of vibration. Figure 17 shows R_0 plotted as a function of frequency. Although three runs were made at 90°F, 95°F, and 100°F, it was observed that R_0 was not a function of temperature and a very weak function of the frequency of vibration.

The values of R_0 for each frequency of vibration was then used in the computer program to calculate thermal conductivity, K_L, as shown by the equation:

$$K_L = \Delta X/(R_T - R_0)A = Q\Delta X/A\Delta T.$$

Measurement of Thermal Conductivity as a Function of Frequency

The individual values of thermal conductivity were determined and plotted as a dimensionless ratio K_F/K_S. This is the thermal

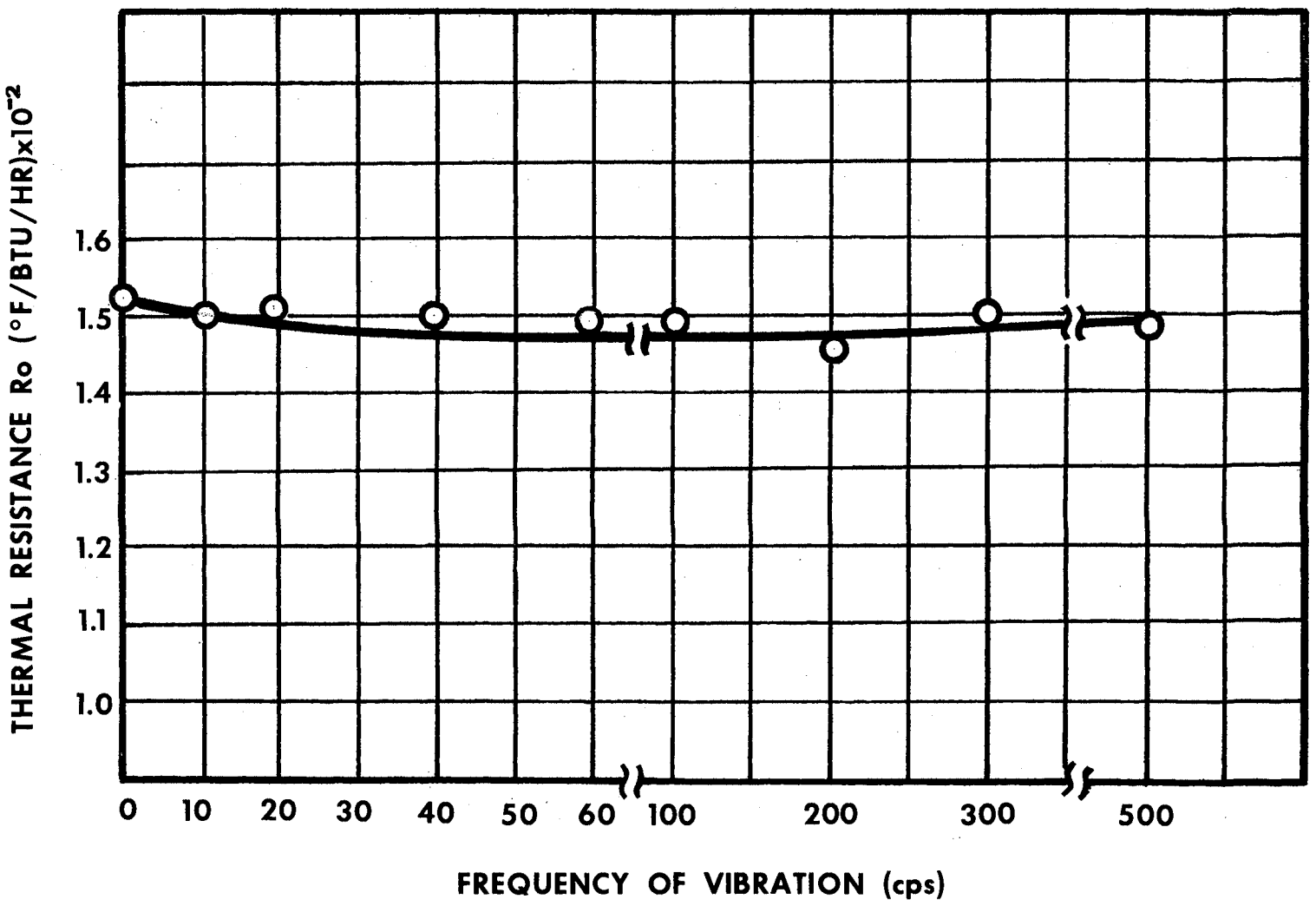

FIGURE 17—VALUES OF Ro VERSUS FREQUENCY

conductivity at some frequency F divided by the thermal conductivity under static conditions or F = 0. The results were plotted for each film thickness and will be discussed individually.

Film Thickness 0.600

The response to frequency of vibration was manifested only between the limits zero to twenty-five CPS. The lowest frequency at which 1.0 G force could be imposed was 6.30 CPS. Figure 18 shows a maximum increase of 6.2 percent at the 7.0 CPS point. All frequencies above 30 CPS show virtually no response to frequency of vibration.

Film Thickness 0.500

The response of thermal conductivity was very similar to the previous case of 0.600. The influence was manifested between zero and twenty CPS with maximum response at 8.0 CPS. The data shows an 11 percent increase over static values.

Film Thickness 0.400

The response curve shows maximum increase at 8.0 CPS with a 7 percent increase over static values. Also, no influence in values of thermal conductivity was noted above twenty-five CPS.

Film Thickness 0.300

The response curve exhibited basically the same behavior, with maximum influence at 9.5 CPS, and a 5.5 percent increase.

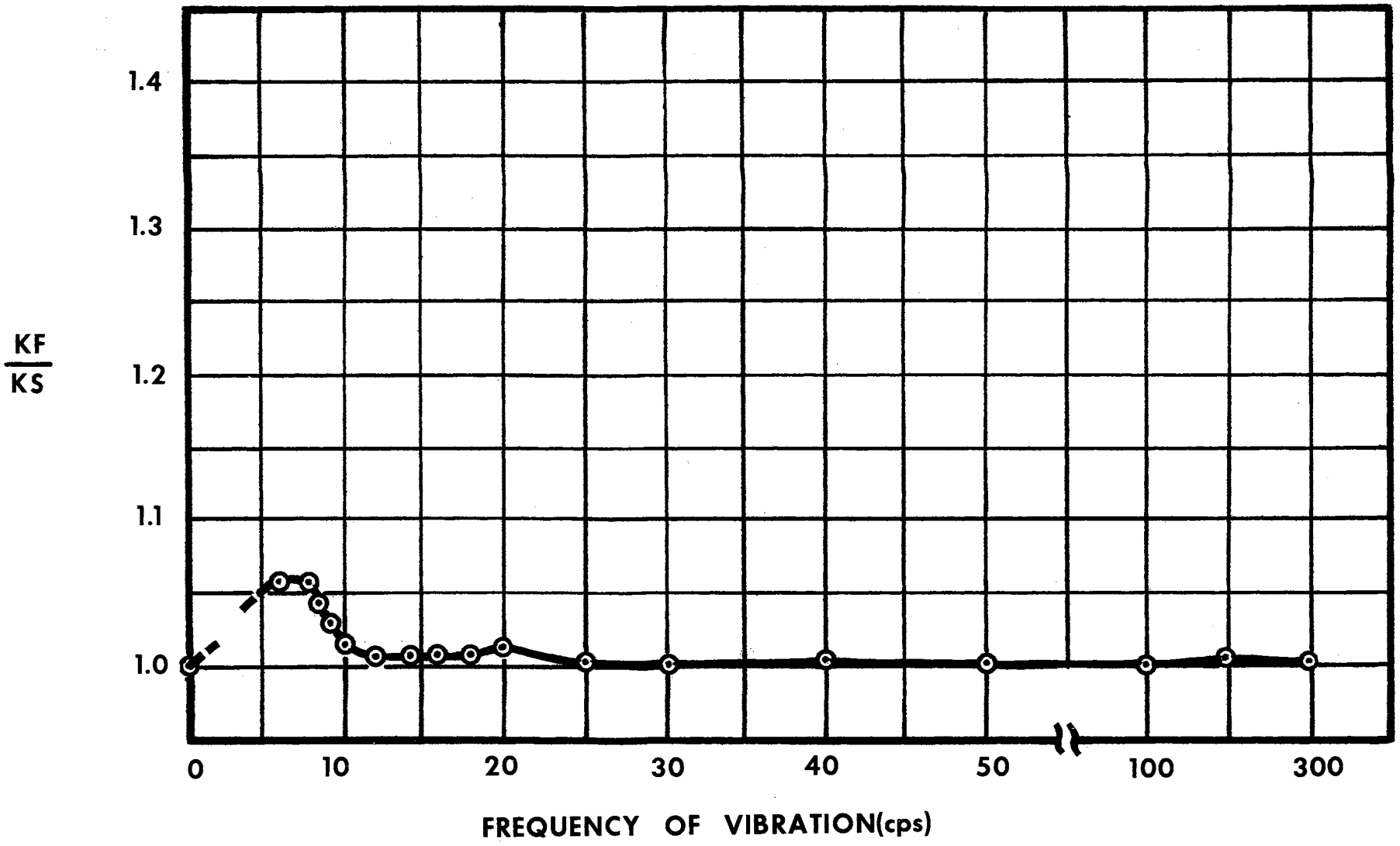

FIGURE 18— KF/KS VS FREQUENCY FOR FILM THICKNESS OF 0.600 INCHES

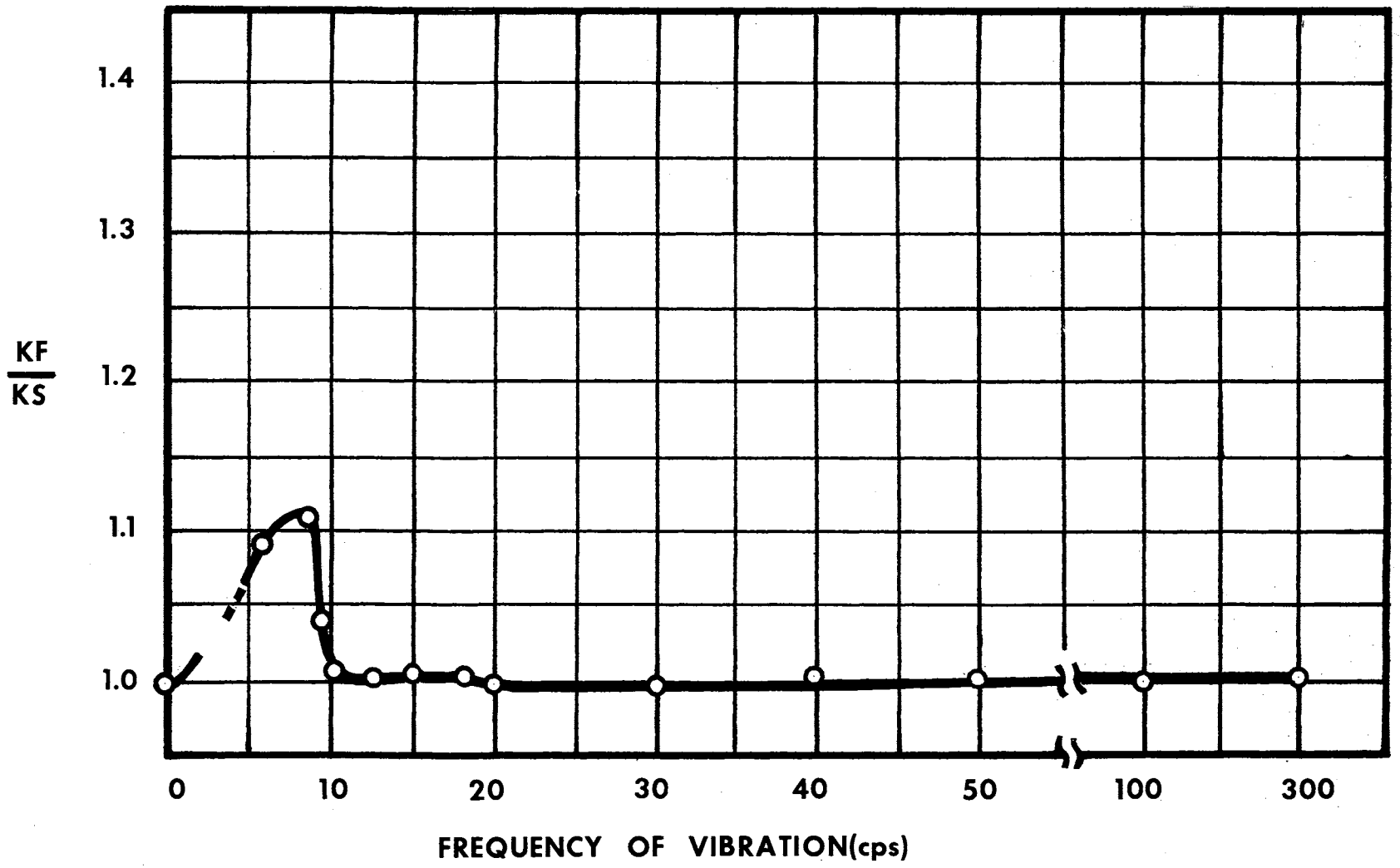

FIGURE 19—KF/KS VS FREQUENCY FOR FILM THICKNESS OF 0.500 INCHES

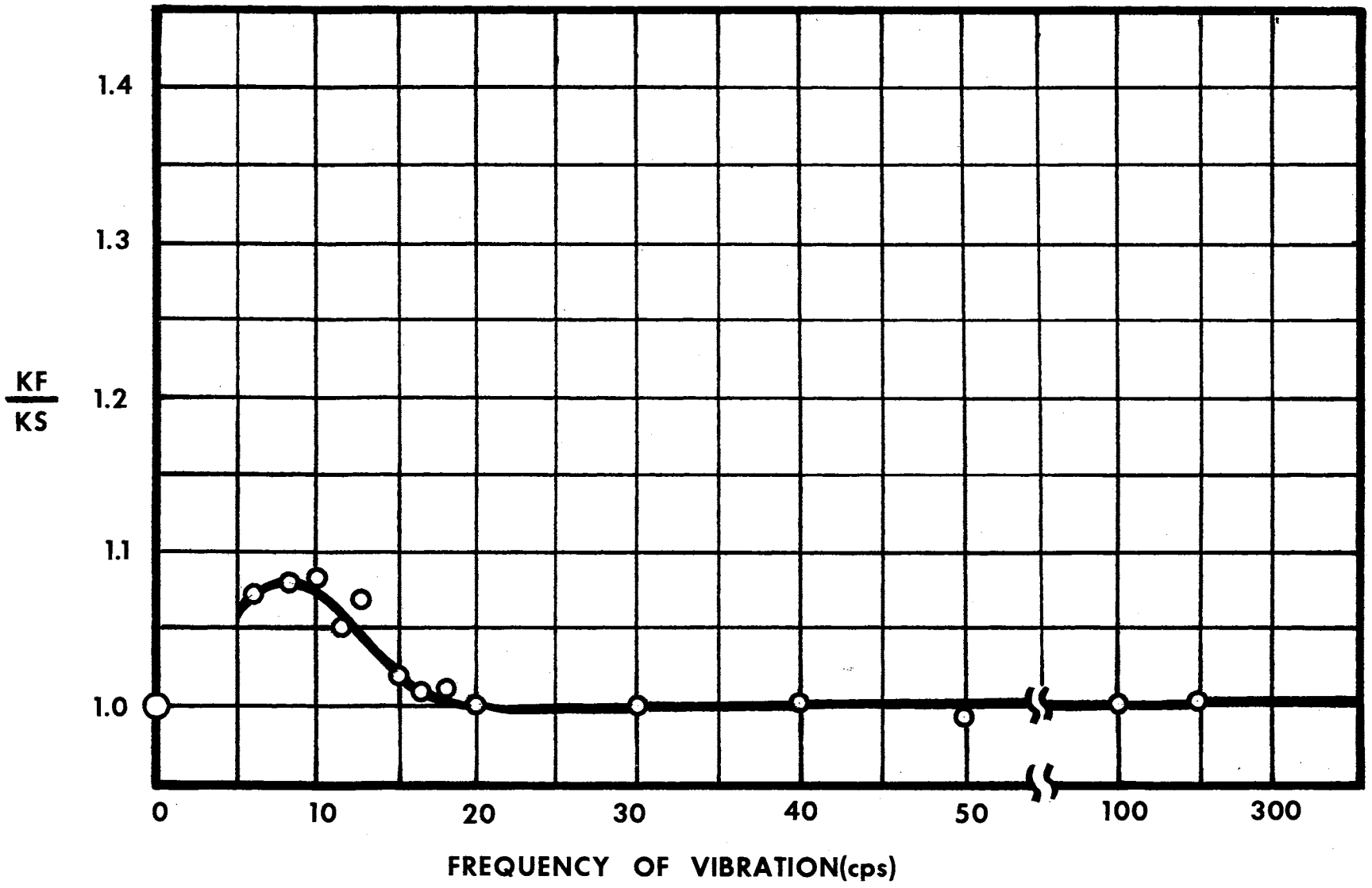

FIGURE 20—KF/KS VS FREQUENCY FOR FILM THICKNESS OF 0.400 INCHES

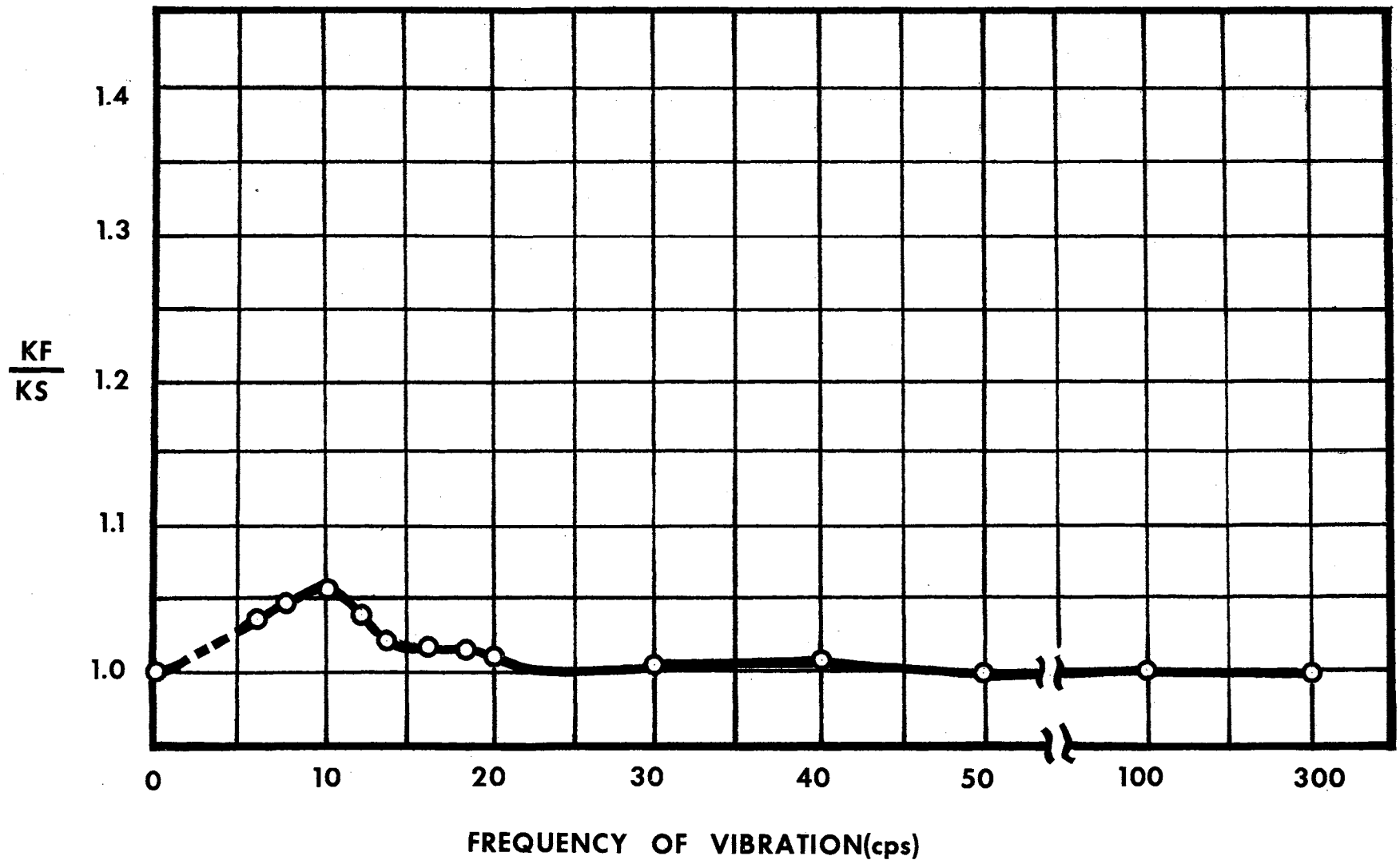

FIGURE 21—KF/KS VS FREQUENCY FOR FILM THICKNESS OF 0.300 INCHES

Film Thickness of 0.200

The response curve indicates a trend toward slightly higher frequencies as film thickness decreases. In the 0.200 film thickness, the frequency of maximum response has shifted to 12.5 CPS with the identical maximum amplitude of 5.5 percent.

Film Thickness 0.100

The maximum response is evident at the slightly higher frequency of 14.0 CPS. The amplitude remains constant at approximately 5.0 percent increase.

Measured Values of Thermal Conductivity with Increase in Force of Acceleration

An additional test run using the 0.600 inch film thickness was reaccomplished the next day following the completion of the normal test run. This run was specifically to determine the repeatability of the data and to determine the variation of thermal conductivity for G levels of 1.0 G, 2.0 G, and 3.0 Gs. The values for the dimensionless ratio KF/KS are shown in Figure 24. The response to frequency for this run traced an almost identical path to the previous run and the values for 1.0 G, 2.0 G, and 3.0 G trace almost identical curves.

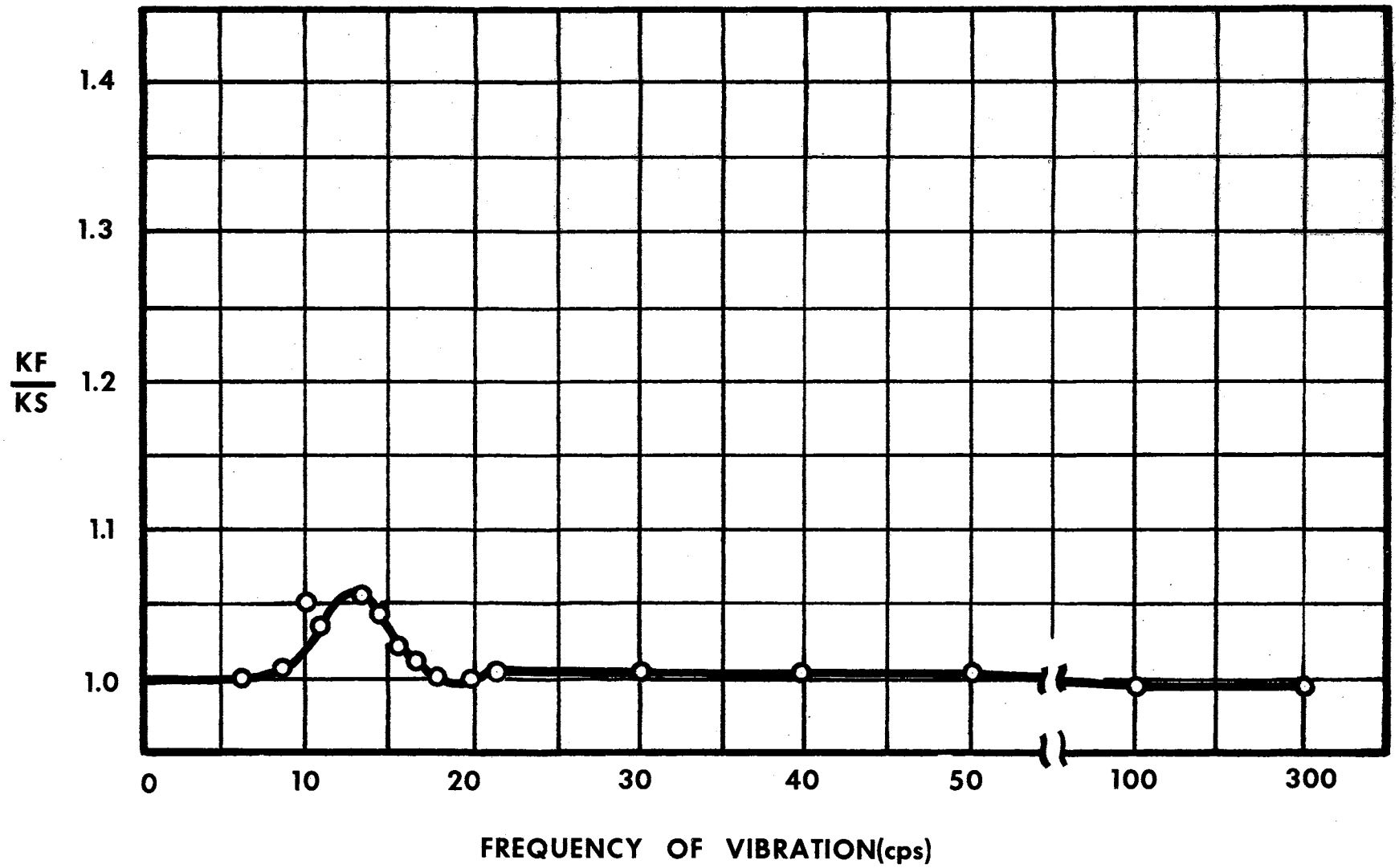

FIGURE 22—KF/KS VS FREQUENCY FOR FILM THICKNESS OF 0.200 INCHES

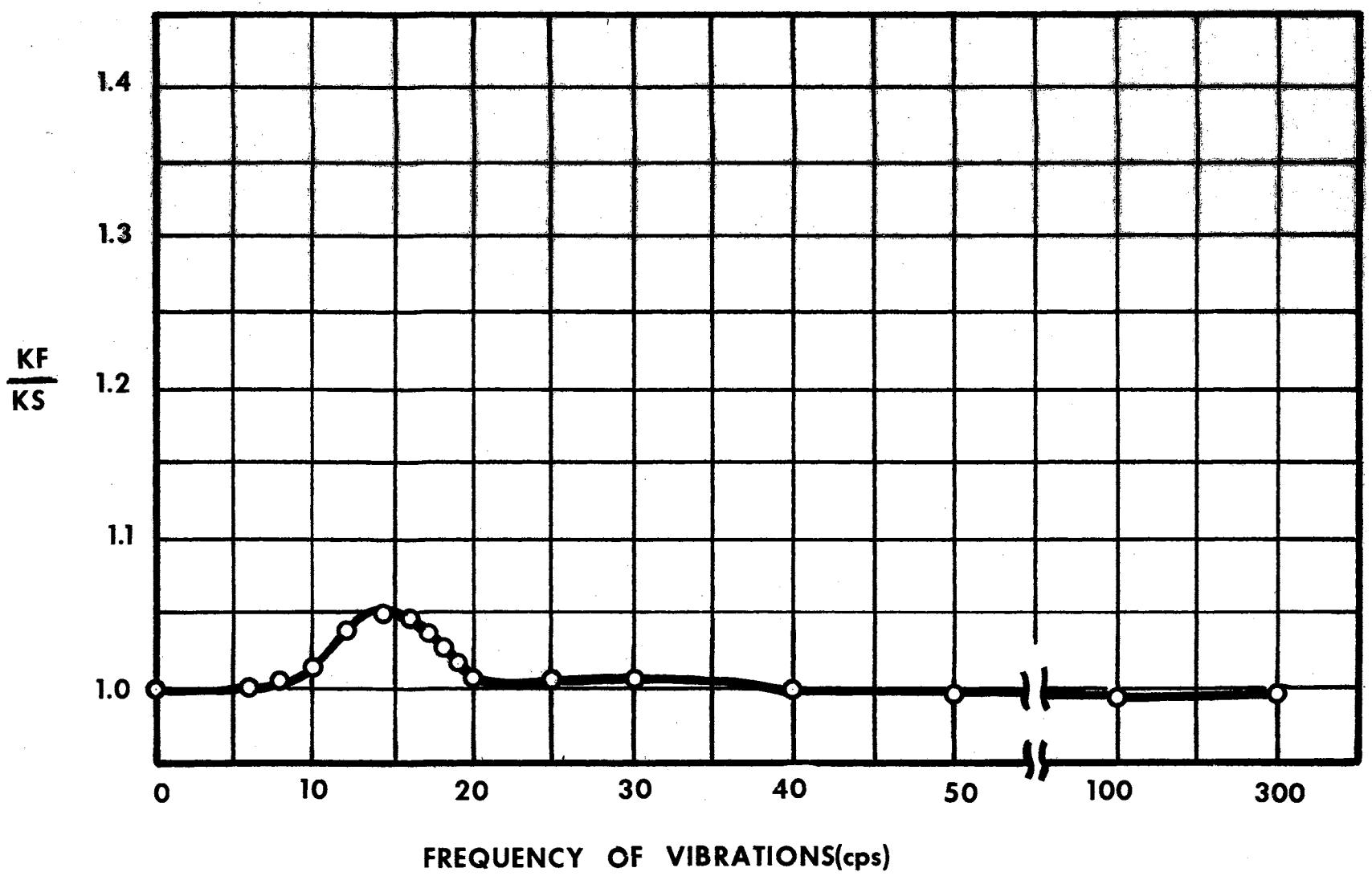

FIGURE 23—KF/KS VS FREQUENCY FOR FILM THICKNESS OF 0.100 INCHES

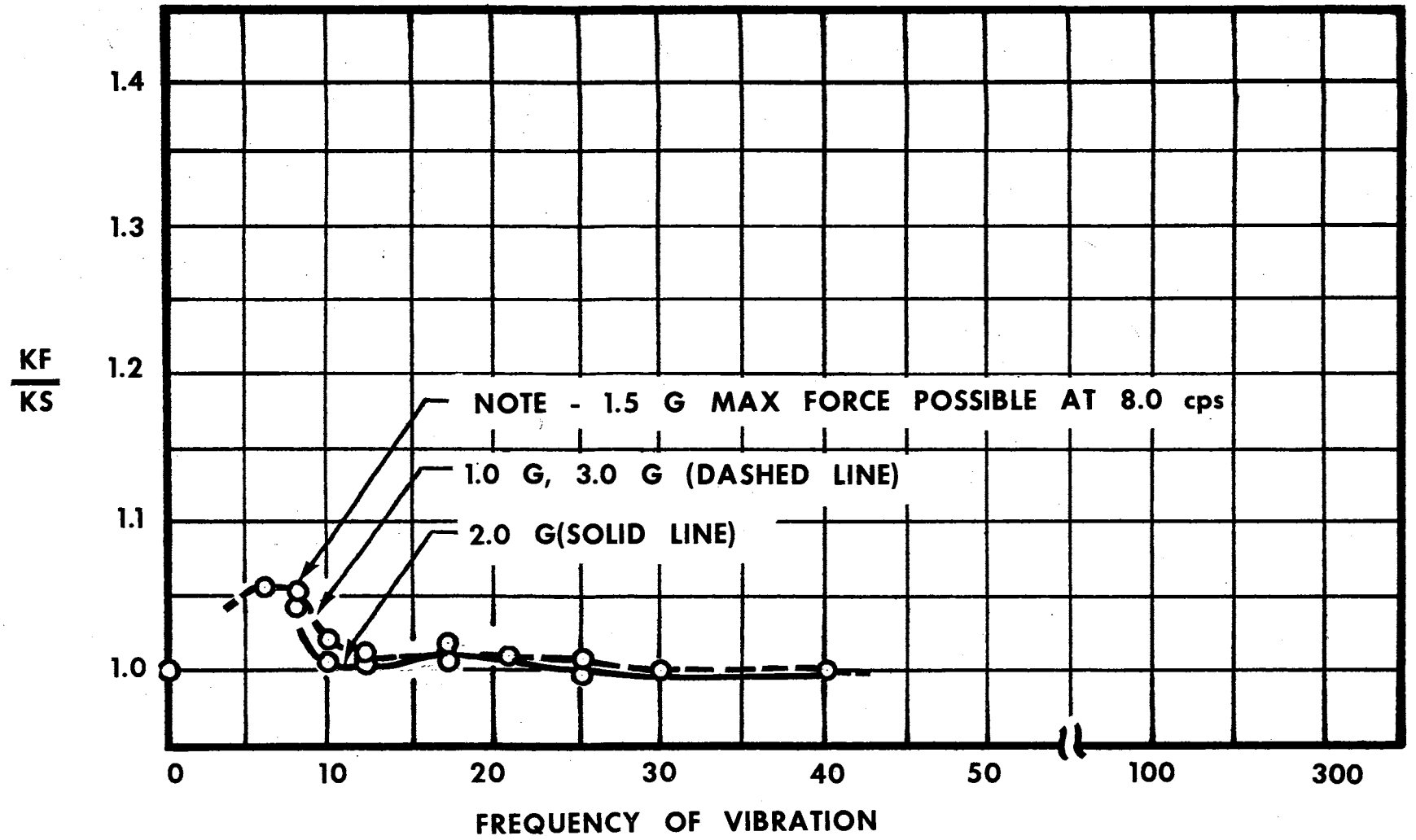

FIGURE 24—KF/KS VS FREQUENCY FOR FILM THICKNESS OF 0.600 INCHES WITH VARIABLE 'G' FORCE

Visible Phenomena

Numerous tests were conducted to detect the presence of any visible phenomena. During test runs the chamber was under continuous observation to detect the onset of any visible phenomena but none was detected. After the data runs were completed, spherical latex particles of 50-100 micron size, with a density of water, were injected into the test chamber. This represented an attempt to photograph the possible occurrence of convection patterns within the liquid test sample. The test sample was vibrated at the frequency of maximum response, as determined earlier. Film strips using high speed photography were made and every 100th frame was collected and a composite formed. However, after careful study the composite failed to reveal any pattern of the latex particles. The only motion of the latex particles could be described as a gentle random motion with adherence to no particular pattern. The latex particles would remain suspended for approximately two minutes then gently settle to the bottom or rise to the upper surface.

Comparison of Data

The values of thermal conductivity measured under static condition (K_S) are given in Table III.

TABLE III

Film Thickness (inches)	K_S	Percent Deviation From Mean Value
0.100	0.3456	+2.31
0.200	0.3208	-6.96
0.300	0.3419	-0.84
0.400	0.3731	+8.20
0.500	0.3400	-1.16
0.600	0.3127	-9.25

The mean value of K_S for all film thicknesses was 0.3448. The values of thermal conductivity for 93°F in Figure 1 range from 0.3370 to 0.3460. The deviations from the mean value can only be explained as attributable to factors not accounted for in the calculation of maximum uncertainty, such as contamination of liquid sample and human error.

CHAPTER VI

CONCLUSIONS AND RECOMMENDATIONS

The following conclusions have been reached from the results of this study.

a. The thermal conductivity of distilled water is increased when influence by a sinusoidal vibration in the frequency ranges of zero to approximately twenty-five cycles per second.

b. The increase of the force of acceleration, up to 3.0 G, appears to have no effect on measured values of thermal conductivity.

c. The increase in thermal conductivity is not associated with any detectable flow pattern within the test layer.

d. The increase in thermal conductivity varied from 5.0 percent with a film thickness of 0.100 inches to 11.0 percent at 0.500 inches.

e. The frequency of maximum response varied from 14.0 CPS at 0.100 inches of film thickness to 6.3 CPS at 0.600. The frequency of maximum response varied inversely to film thickness.

Recommendations for Future Study

It is doubtful if further work in this specific area would be of any industrial significance. However, in the interest of basic research and to increase the understanding of heat transfer properties

of liquids and their relationship to the molecular structure, the following recommendations are made for further study.

1. That experimental work be accomplished in applying a vibratory force perpendicular to the direction of heat transfer. This is to investigate the effect of vibratory relative motion at the liquid-metal interface.

2. That liquids of different viscosities be investigated to determine effect of viscosity upon frequency of vibration at which maximum response occurs.

A SELECTED BIBLIOGRAPHY

(1) Mason, H. L. "Thermal Conductivity of Liquids from 0 to 100°C." Trans. Amer. Soc. Mech. Engrs. Vol. 76. (1954) 817.

(2) Jacob, M. "Determination of the Heat Transfer of Liquids in the Range of 0-80°. Ann. Physics. Leipzig. Vol 63 (1920) 537.

(3) Smith, J. F. D. "Thermal Conductivity of Liquids." Industr. Engng. Chem. Vol 22 (1930) 1246-1252.

(4) Euchen, A. and E. Englert. "Determination of Thermal Conductivity of Liquids." Z. ges. Kalteind. Vol 45 (1938) 109.

(5) Riedel, L. "Warmeleitfahrigkeitsmessungen an flussigkeiten." Mitt. Kaltetech. Inst. Karlsruhe. Vol. 2 (1948).

(6) Kardos, A. "Studies of Thermal Conductivities of Liquids." Ver. dtsch. Ing. Vol 77 (1933) 1158.

(7) Hutchinson, E. "Heat Transfer of Fluids." Trans. Faraday Soc. Vol 41 (1945) 87.

(8) Stalhane, J. B. and S. C. Pyk. "Production of Alkali Metals by Electrolysis of Fused Salts." Swed. Vol. 72 (1931) 843.

(9) Pfriem, J. K. "Apparatus for Determination of Thermal Conductivity." Physica. Vol 29 (1932) 747-749.

(10) Weishaupt, J. "Heat Transfer of Liquids." Forsch. Ing. Wes. Vol. 11 (1940) 20.

(11) van der Held, E. F. M. and F. G. van Drunen. "A Method of Measuring the Thermal Conductivity of Liquids." Physica. Vol. 19 (1949) 856.

(12) Martin, L. H. and K. C. Lang. "Thermal Conductivity of Water." Proc. Phys. Soc. Vol. 45 (1933) 523-529.

(13) Bates, O. K., G. Hazzard, and G. Palmer. "Thermal Conductivity of Liquids." Indust. & Engin. Chem. (Analytical Edition). Vol. 10 (June 15, 1938) 314-318.

(14) Bridgman, P. W. "Thermal Conductivity of Liquids under Pressure." Proc. Amer. Acad. Arts. Sci. Vol 5. (1923) 141-169.

(15) Smith, J. F. D. "Thermal Conductivity of Liquids." Industr. Engng. Chem. Vol 22. (1930) 1246.

(16) Daniloff, M. "Thermal Conductivity of the Normal Primary Saturated Alcohols." J. Amer. Chem. Soc. Vol 54. (1932) 1328.

(17) Schmitt, E., and W. Sellschopp. "Thermal Conductivity of Liquids." Forsch. Ing. Wes. Vol. 2 (1932) 277.

(18) Schrock, V. E. and E. S. Starkman. "Spherical Apparatus for Measuring the Thermal Conductivity of Liquids." The Review of Scientific Instruments. Vol. 29. (1958) 625-629.

(19) Sakiadis, B. C. and J. Coates. "Studies of Thermal Conductivity of Liquids." Engineering Experiment Station, Louisiana State University. Bulletin No. 45 (1955).

APPENDIX A

LIST OF SYMBOLS

HPBT	A group of four thermocouples used to measure the heater element Bottom Plate Temperature.
CPLT	A group of four thermocouples used to measure the Cold Plate Temperature.
HPTT	A group of four thermocouples used to measure the Hot Plate Top Temperature.
TPGT	A group of four thermocouples used to measure the Top Plate Guard Temperature.
HPGT	A group of four thermocouples used to measure the Hot Plate Guard Temperature.
Q(IN)	The total amount of heat supplied to the heater element.
e_h	Potential (volts) across the heater element.
R_S	Resistance of precision shunt.
R_{ST}	Resistance of precision shunt at temperature T.
R_L	Resistance of lead wires.
R_{LT}	Resistance of lead wires at temperature T.
VDR	Voltage divider ratio.
i_h	Current through heater element loop.
Q(L)	Sum of heat loss by heater element other than through test liquid.
Q(COR)	Amount of heat transferred through liquid sample by conduction.
R_0	Residual resistances measured when separation of plates is zero.

R_T	Total resistance of liquid to heat transfer by conduction.
K_L	Thermal conductivity of liquid corrected for residual resistance R_O.
TI	Temperature measured on inside surface of test chamber.
TO	Temperature measured on outside of test chamber.
ΔX	Linear separation between hot surface and cold surface. It is also the thickness of liquid test sample.
ΔT	Temperature difference between adjacent metal surfaces.

APPENDIX B

LIST OF MAJOR INSTRUMENTATION

Mueller Bridge--Model 1551; Manufacturer, Rubicon; Serial No. 119883.

Platinum Resistance Thermometer--Model 8163; Manufacturer, Leeds and Northrup; Serial No. 1613906.

Potentiometer--Model K-2; Manufacturer, Leed and Northrup.

Potentiometer--Model B; Manufacturer, Rubicon; Serial No. 77183.

Galvanometer--Model 2100; Manufacturer, Leeds and Northrup.

Constant Temperature Oil Bath--Model 4-1257; Manufacturer, American Instrument Co.; Serial No. 15247.

Vibration Test Equipment:

Control Equipment--Model 45A; Manufacturer, Calidyne.

Shaker System--Model B44; Manufacturer, Calidyne.

Charge Amplifier--Model 568; Manufacturer, Kistler; Serial No. SJN 201.

Accelerometer--Model 2215; Manufacturer, Endevco Corp.; Serial No. 7626.

Accelerometer--Model 2215; Manufacturer, Edevco Corp.; Serial No. 7641.

Microvolt Potentiometer--Model 2768; Manufacturer, Honeywell Inc.; Serial No. 115651.

Voltage Divider--Model 4395; Manufacturer, Leeds and Northrup Serial No. 1526540.

Galvanometer--Model 2430-C; Manufacturer, Leeds and Northrup.

Strip Chart Recorder--Electronik 17; Manufacturer, Honeywell; Serial No. 260657001.

Strip Chart Recorder--Electronik 17; Manufacturer, Honeywell;
Serial No. L000855A.

Vacuum Tube Voltmeter--Hewlett-Packard; Serial No. 265.

EPUT Timer--Model 7360; Manufacturer, Beckman-Berkley; Serial No. 5567.

Charge Amplifier--Model 568; Kistler; Serial No. 152.

Storage Oscilloscope--Type 564; Tektronix; Serial No. 009990.

Power Supply-DC Regulated--Model 810B-X; Harrison Laboratories.

APPENDIX C

CALIBRATION OF THERMOCOUPLES

The purpose of conducting an extensive calibration of the thermocouples was to determine the accuracy and reliability of the thermocouples and the temperature measuring circuitry.

Although the measurement of thermal conductivity depends on ΔT, there are several valid reasons for determining ΔT from

$$\Delta T = T \text{ (hot)} - T \text{ (cold)}$$

rather than measuring the difference in emf and converting to difference in temperature.

Greater accuracy can be realized in measuring the emf of T (hot) and that of T (cold) rather than the emf of ΔT due to the unreliability and unstability of small emf reading on most potentiometers.

It was also felt that if the temperature-emf curve from the thermocouple calibration compared favorably with that published by the National Bureau of Standards for Copper-Constantan thermocouples; the measuring system as well as the thermocouples themselves could be considered acceptable.

Deviations in the temperature-emf curve from that of the National Bureau of Standards would indicate the presence of either systematic errors or accidental errors, and a comparison of the two curves would indicate if either was present as well as approximate magnitude.

Also such a comparison would indicate the homogeneity in the thermocouples.

Another valid reason is the important observation that emf V_s temperature relationship is not linear, therefore, emf is a function of temperature absolute.

The schematic for calibration apparatus is shown in Figure 6. The thermocouple elements were formed into 6 groups of 8 thermocouple elements in each group, 4 for reference temperature and 4 for temperature measurement. The thermocouple elements were connected directly to copper lead wires which were in turn connected to a 24 position thermocouple switch. The switch and junctions were thermally insulated to avoid difference in temperature.

To assure an accurate ice point reference considerable attention was directed toward the construction and use of a DeWar Flask. Distilled water was frozen, chipped into very small pieces and placed in the DeWar Flask. The flask was filled with sufficient pure distilled water to just fill the interstices of the ice. An insulating cover with six openings for the placement of nine inch test tubes covered the DeWar Flask.

Each test tube was filled with kerosene. A minimum of six inches of thermocouple wire was immersed in the kerosene and moisture-free cotton insulation was placed around the thermocouple wire. A maximum of four well lacquered junctions were immersed in each test tube of kerosene. This formed the reference junction for each thermocouple pair.

The measurement junctions of each thermocouple pair were taped to the outside periphery of the Platinum Resistance Thermometer probe,

which was placed in a large test tube filled with oil which was in turn placed in the constant temperature oil bath. The oil bath temperature was thermostatically controlled and accurate to ±0.01°F. The test tube acted as a buffer to reduce cyclic changes in temperature of the oil within the test tube.

The instrumentation was arranged to provide simultaneous reading of a Mueller Bridge and a Rubicon Potentiometer. The Mueller Bridge balance as indicated by the sliding scale Galvanometer indicated an accurate reading of the Platinum-Resistance Thermometer, readable to 0.0001 ohms.

The Rubicon Potentiometer provided an accurate reading of the emf of the thermocouple circuit readable to 1.0 microvolt and interpolated to 0.1 microvolt. The potentiometer was checked frequently to insure the stability of the constant voltage source, a six volt dry cell battery, by checking against an accurately calibrated standard cell. The Rubicon Potentiometer was repeatedly checked against a K-2 Leeds and Northrup Potentiometer, readable to 0.1 microvolts, calibrated by the National Bureau of Standard.

A No. 2284A, Type HS, Leeds and Northrup Reflecting Galvanometer, with a sensitivity of 0.44 microvolts per mm at a distance of 1 meter, two Eppley standard cells, a 6 volt dry-cell storage battery, an instrument panel containing a 24 point thermocouple selector switch completed the necessary calibration equipment.

The room temperature and equipment temperature were allowed to stabilize for approximately six hours before data was taken. The 24 position thermocouple switch and junction panel was heavily insulated to insure isothermal conditions throughout the switching circuit.

The resistance of the Platinum Resistance Thermometer was carefully measured while the probe was immersed in the ice bath reference (DeWar Flask). This determined the value of R_0. Stabilization was attained for at least 10 minutes before any readings were taken. The resistance was read in the "Forward" position, then "Reverse" and the readings averaged to determine the value of R_0.

The thermocouples were calibrated in the range of 40°C - 80°C in 5° intervals. The following step-by-step procedure was adapted for the calibration.

a. Oil bath at proper temperature and stabilized as indicated by the heater light "out" and "on" only during cyclic heating to maintain ±.01°F.

b. The Rubicon Potentiometer checked against standard cell.

c. K-2 Potentiometer checked against standard cell.

d. Thermocouple switch position noted.

e. Mueller Bridge balanced to read exactly "zero" and the galvanometer "Forward" and "Reverse" readings carefully noted while simutaneously the Rubicon Potentiometer was balanced and readings taken. This simultaneous procedure, made possible by two operators, precluded variations in readings due to cyclic changes of the oil bath temperature.

A minimum of two readings for each thermocouple group, or thermopile, and two for each individual pair, read individually, was recorded.

The "Forward" and "Reverse" readings were averaged to yield R_0, the resistance in ohms of the Platinum Resistance Thermometer pertaining to a particular temperature. This procedure was repeated for each temperature change of 5°C. The data, R_p (ohms) was reduced to temperature (°F) utilizing an IBM 1620 computer program.

The resulting temperature (°F) versus emf relationship for each thermocouple group was further reduced by a curve fitting technique by an IBM 1620 computer program (see Appendix F).

The result of this program represents a curve which best fits the points of temperature (°F) versus emf. Computer programming also calculated the error of each point from this "ideal" curve in degrees Fahrenheit as a basis of further comparison and evaluation. A curve using values from tables of the National Bureau of Standards was also used as the ideal curve to evaluate these points. The composite tabulation is presented in Table IV.

A curve that provided the best fit of the data points was obtained when the value of emf appeared raised to the second power. Although the highest value of the exponent was tried for values one through six, the quadratic form presented the best curve fit.

$$\text{Temperature} = A + B(\text{emf}) + C(\text{emf})^2$$

where

$$A = -0.071336281$$

$$B = 0.021175591$$

$$C = 0.000011029$$

yielded the best curve for all points.

The values of temperature versus emf from the National Bureau of Standards for Copper-Constantan also yielded a best fit when the curve was of the quadratic form.

$$\text{Temperature} = A + B(\text{emf}) + C(\text{emf})^2$$

where

$$A = -0.68039537$$

$$B = 0.020706857$$

$$C = 0.000012698$$

The calibration data compared to this curve appears in Column 6 designated **.

A close examination of the calibration data reveals that all groups had a maximum deviation of ±0.063°F when compared to the standard curve of

$$\text{Temperature} = -0.071336281 + 0.021175591(\text{emf}) + 0.000011029(\text{emf})^2$$

TABLE IV

THERMOCOUPLE CALIBRATION DATA

GROUP 1

Oil Bath Temperature	Thermocouple emf	Δemf	ΔTemperature (°F) *	ΔTemperature (°F) **
110.5995	1.7668	0.00129	0.05495	0.12373
120.3195	1.9954	0.00019	0.00824	0.08449
127.9885	2.1772	-0.00091	-0.03826	0.04017
137.4083	2.4038	-0.00084	-0.03508	0.04169
143.9611	2.5643	0.00081	0.03357	0.10227
153.9742	2.8082	0.00002	0.00094	0.06347
161.3613	2.9918	0.00156	0.06331	0.11491
170.3399	3.2120	-0.00126	0.05089	-0.01586
178.9607	3.4330	0.00376	0.14984	0.16466

* Values plotted against "Best-Fit" curve - "Sum Of Least Squares," IBM 1620 computer program - using values from calibration data (Column 1 and 2).

** Values plotted against curve data extracted from tables published by National Bureau of Standards, Washington, D. C. However, it is important to note that tabulated values of NBS are published for 3 decimal places only, whereas values from calibration data are presented for 4 decimal places.

TABLE IV (continued)

GROUP 2

Oil Bath Temperature	Thermocouple emf	Δemf	ΔTemperature (°F) *	ΔTemperature (°F) **
110.5995	1.7668	0.00129	0.05495	0.12373
120.3195	1.9954	0.00019	0.00824	0.08449
127.9885	2.1772	-0.00091	-0.03826	0.04017
137.4083	2.4038	-0.00084	-0.03508	0.04169
143.9611	2.5643	0.00081	0.03357	0.10227
153.9742	2.8082	0.00002	0.00094	0.06347
161.3613	2.9918	0.00156	0.06331	0.11491
170.3399	3.2120	-0.00126	-0.05089	-0.01586
178.9480	3.4300	0.00108	0.04328	0.05839

TABLE IV (continued)

GROUP 3

Oil Bath Temperature	Thermocouple emf	Δemf	ΔTemperature (°F) *	ΔTemperature (°F) **
110.6452	1.7670	0.00041	0.01775	0.08654
120.3195	1.9954	0.00019	0.00814	0.08449
127.9885	2.1772	-0.00091	-0.03826	0.04017
137.4083	2.4038	-0.00084	-0.03508	0.04169
143.9611	2.5643	0.00081	0.03357	0.10227
153.9742	2.8082	0.00002	0.00094	0.06347
161.3613	2.9918	0.00156	0.06331	0.11491
170.3399	3.2120	-0.00126	-0.05089	-0.01586
178.9480	3.4300	0.00108	0.04328	0.05839

TABLE IV (continued)

GROUP 4

Oil Bath Temperature	Thermocouple emf	Δemf	ΔTemperature (°F) *	ΔTemperature (°F) **
110.6452	1.7670	0.00041	0.01775	0.08654
120.3195	1.9954	0.00019	0.00824	0.08449
127.9885	2.1772	-0.00091	-0.03826	0.04017
137.4083	2.4038	-0.00084	-0.03508	0.04169
143.9611	2.5643	0.00081	0.03357	0.10227
153.9742	2.8082	0.00002	0.00094	0.06347
161.3613	2.9918	0.00156	0.06331	0.11491
161.3613	2.9918	0.00156	0.06331	0.11491
178.9262	3.4295	0.00113	0.04521	0.06037

TABLE IV (continued)

GROUP 5

Oil Bath Temperature	Thermocouple emf	Δemf	ΔTemperature (°F) *	ΔTemperature (°F) **
110.5995	1.7668	0.00129	0.05495	0.12373
120.3195	1.9954	0.00019	0.00824	0.08449
127.9885	2.1772	-0.00091	-0.03826	0.04017
137.4083	2.4038	-0.00084	-0.03508	0.04169
143.9611	2.5643	0.00081	0.03357	0.10227
153.9742	2.8082	0.00002	0.00094	0.06347
161.3613	2.9918	0.00156	0.06331	0.11491
170.3399	3.2120	-0.00126	-0.05089	-0.01586
178.9184	3.4284	0.00016	0.00667	0.02194

TABLE IV (continued)

GROUP 6

Oil Bath Temperature	Thermocouple emf	Δemf	ΔTemperature (°F) *	ΔTemperature (°F) **
110.5995	1.7668	0.00129	0.05495	0.12373
120.3195	1.9954	0.00019	0.00824	0.08449
127.9685	2.1772	-0.00091	-0.03826	0.04017
137.4083	2.4038	-0.00084	-0.03508	0.04169
143.9611	2.5643	0.00081	0.03357	0.10227
153.9742	2.8082	0.00002	0.00094	0.06347
161.3613	2.9918	0.00156	0.06331	0.11491
170.2120	3.2120	-0.00126	0.05089	-0.01586
178.9182	3.4291	0.00093	0.03730	0.05251

APPENDIX D

INSTRUMENTATION ERROR FOR CALCULATION OF MAXIMUM UNCERTAINTY

QUANTITY MEASURED	SYMBOL	ACCURACY	METHOD OF MEASUREMENT	CALIBRATION
Temperatures (°F)	CPLT	±0.063	Platinum Resistance Thermo.	National Bureau of Standards
	HPBT	±0.063		
	TPGT	±0.063		
	HPGT	±0.063		
	CPGT	±0.063		
	HPTT	±0.063		
	T0	±0.063		
	T1	±0.063		
	T2	±0.063		
	T3	±0.063		
	T4	±0.063		
	T5	±0.063		

QUANTITY MEASURED	SYMBOL	ACCURACY	METHOD OF MEASUREMENT	CALIBRATION
Temperatures (°F)	TD6	±2.0	Determined for each data run by numerical analysis using known boundary conditions	None
	TD4	±2.0		
	TD2	±2.0		
	T1	±2.0		
	T2	±2.0		
	T3	±2.0		
	T4	±2.0		
	T5	±2.0		
	T6	±2.0		
	T7	±2.0		
	T8	±2.0		
	T9	±2.0		
Potential	EONE	±0.1 Microvolt	Microvolt Potentiometer	Differential Voltmeter Calibrated by National Bureau of Standards
	EMFD	±0.1 Microvolt		
	EMFS	±0.1 Microvolt		

QUANTITY MEASURED	SYMBOL	ACCURACY	METHOD OF MEASUREMENT	CALIBRATION
Linear Distance (inches)	AX1	±0.0005"	Micrometer	Calibration
	AX2	±0.0005"		
	RI	±0.0005"		
	RO	±0.0005"		
Area (sq. ft)	AP	±0.000126	Micrometer	Calibration Block
	AFS	±0.000126		
	ASC	±0.000126		
	ACR	±0.000126		
Resistance (ohms)	RST	±0.000010	Kelvin Bridge	Differential Voltmeter
	RLT	±0.000010		
Voltage Ratio	VDR	±.01%	Differential Voltmeter	Calibrated by N.B.S.
Frequency (Cycles per)	Cps	±0.1%	Accelerometer EPUT meter and Storage Oscilliscope	EPUT meter calibrated against frequency standard which is calibrated by N.B.S.

QUANTITY MEASURED	SYMBOL	ACCURACY	METHOD OF MEASUREMENT	CALIBRATION
Force of Acceleration	G	±.01g	Accelerometer	Calibrated against N.B.S. standard
Force of Acceleration	G	±1% of full scale	Vacuum-Tube Millivoltmeter	

APPENDIX E

PROGRAM FOR CONVERTING PLATINUM RESISTANCE THERMOMETER READINGS L AND N TYPE 8163 TO DEGREES KELVIN, CENTIGRADE, RANKINE, AND FAHRENHEIT

```
      READ 401,A,B,C

      READ 501,RO

      READ 501, ZERO

      READ 502,TOL

      READ 501, TOOL

      READ 501,TOOM

      READ 501,TA

      PAUSE

      TYPE 600

      TYPE 601

1     READ 501,RT
      RA=RT/RO
      IF(RO-RT)2,7,8

2     IF(TA)3,3,5

3     TA=10.0

5     TB+TA*TA
      TC=1.0+(A*TA)+(B*TB)
      SUM=RA-TC
      PHIL=ABSF(SUM)
      IF(PHIL-TOL)13,13,6

6     IF(TC-TOOL)14,15,15

14    TA=TA*(RA/(TC*TC))
      GO TO 5
```

```
15    TA=TA*(RA/TC)
      GO TO 5

7     TYPE 503,RT,ZERO
      GO TO 1

8     IF(TA)10,9,9

9     TA=-10.0

10    TB=TA*TA
      TD=TB*TA
      TE=TB*TB
      TC=1.0+(A*TA)+(B*TB)+(C*TE)-(100.0*C*TD)
      SUM=RA-TC
      PHIL=ABSF(SUM)
      IF(PHIL-TOL)13,13,12

12    IF(TC-TOOM)16,16,17

16    TA=TA*(TC/RA)
      GO TO 10

17    TA=TA*((TC*TC)/RA)
      GO TO 10

13    TK=273.15+TA
      TR=1.80*TK
      TF=TR-459.670
      TYPE 503,RT,TK,TA,TR,TF

401   FORMAT(E20.8,E20.8,E20.8)

501   FORMAT(F10.5)

502   FORMAT(F10.7)

503   FORMAT(F10.4,F10.4,F10.4,F10.F,F10.4)

600   FORMAT(4X,6HBRIDGE,14X,11HTEMPERATURE)

601   FORMAT(3X,7HREADING,4X,6HDEG. K,4X,6HDEG. C,4X6HDEG. R,4X,5HDEG F)

      END
```

APPENDIX F

REGRESSION PROGRAM

```
889  READ110,NVAR,NPTS, C(1),C(2),C(3),C(4),C(5),C(6)

110  FORMAT(I3,I3,F10.5,F10.5,F10.5,F10.5,F10.5,F10.5)
     DO 111 I= 1,NPTS,3

111  READ 112,XA(I),YA(I),XA(I+1),YA(I+1),XA(I+2),YA(I+2)

112  FORMAT(F10.5,F10.5,F10.5,F10.5,F10.5,F10.5)
     GO TO 910

898  READ 891,NVAR,NPTS,MK(1),MK(2),MK(3),MK(4),MK(5),MK(6)

891  FORMAT(I5,I5,I5,I5,I5,I5,I5,I5)
     DO 892 I-1,NPTS,3

892  READ 112,XA(I),YA(I),XA(I+1),YA(I+1),XA(I+2),YA(I+2)
     DO 131 I = 1,NVAR
     DO 131 J = I,NVAR
     A(I,J)= 0.0
     DO 151 K = 1,NPTS

151  A(I,J) = XA(K)**(MK(I)+MK(J)) + A(I,J)

131  A(J,I) = A(I+J)
     KEY = NVAR + 1
     DO 171 I + 1, NVAR
     A(I,KEY) = 0.0
     DO 171 J = 1,NPTS

171  A(I,KEY) = A(I,KEY) + YA(J)*XA(J)**MK(I)
     GO TO 132

910  DO 130 I = 1,NVAR
     DO 150 J + I,NVAR
     A(I,J) + 0.0
     DO 150 K = 1, NPTS

150  A(I,J) + XA(I)**(C(I)+C(J))+A(I,J)
```

```
   30 T(I,1) = A(I,1)
      T(1,1) = 1.0
      DO 40 I = 2,KEY

   40 T(1,I) = A(1,I)/A(1,1)
      I = 1

   61 I = I + 1
      DO 70 J = I,NVAR
      T(J,I) = A(J,I)
      M = I - 1
      DO 70 L = 1,M

   70 T(J,I)=T(J,I) - T(J,L)*(T(L,I))
      IM = I + 1
      DO 80 J = IM,KEY
      T(I,J) = A(I,J)/ T(I,I)
      N1 = I - 1
      DO 80 L = 1,N1

   80 T(I,J) = T(I,J) - T(I,J))/ T(I,I)
      IF(NVAR - I)85,85,61

   85 A(3,NVAR) = T(NVAR,KEY)
      IZZ = NVAR-1
      IF(IZZ)1000,1001,1000

 1000 DO 90 I = 1,IZZ
      K = NVAR - 1
      L = K + 1
      DO 90 J = L, NVAR

   90 A(3,K) = A(3,K)-A(3,J)*T(K,J)

 1001 DO 887 I = 1,NVAR
      IF (SENSE SWITCH 1)886,885

  885 PRINT 98, I, A(3,I),MK(I)

   98 FORMAT(2HA(I3,4H) = E10.5,10X,16HEXPONENT OF X = I3)
      GO TO 887

  886 PRINT 97,I,A(3,I,C(I)

   97 FORMAT(2HA(I3,4H) = E10.5,10X,16HEXPONENT OF X = F8.4)

  887 CONTINUE
      IF(SENSE SWITCH 2)881,880

  881 DO 879 I = 1,NVAR

  879 PUNCH 882,A(3,I)

  882 FORMAT(E14.8)
```

```
880     A(1,4) = 0.0
        IF(SENSE SWITCH 3) 701,702

701     IF (SENSE SWITCH2)841,840

841     PUNCH 6
        GO TO 878

840     PRINT 6

  6     FORMAT(/4X2H X,13X2H Y,10X6H YCALC,6X6H DELTA,6X6H DELII /)

702     CONTINUE

878     IF (SENSE SWITCH 1) 901,902

901     DO 180I = 1,NPTS
        A(1,1) = 0.0
        DO 190 J = 1,NVAR

190     A(1,1) = A(3,J)*XA(I)**C(J)+A(1,1)
        A(1,2) = YA(I) -A(1,1)
        A(1,3) = A(1,2)**2
        A(1,4) = A(1,4) + A(1,3)
        IF (SENSE SWITCH 3)890,180

890     IF(SENSE SWITCH2)876,877

876     PUNCH 202,XA(I),YA(I),A(1,1),A(1,2),A(1,3)
        GO TO 180

877     PRINT 202,XA(I),YA(I),A(1,1),A(1,2),A(1,3)

180     CONTINUE
        GO TO 203

902     DO 181 I = 1,NPTS
        A(1,1) = 0.0
        DO 191 J = 1,NVAR

191     A(1,1) = A(3,J)*XA(I)**MK(J) + A(1,1)
        A(1,2) = YA(I) - A(1,1)
        A(1,3) = A(1,2)**2
        A(1,4) = A(1,4) + A(1,3)
        IF (SENSE SWITCH 3)830,181

830     IF (SENSE SWITCH 2) 874,875

874     PUNCH 202, XA(I),YA(I),A(1,1),A(1,2),A(1,3)
        GO TO 181

875     PRINT 202, XA(I),YA(I),A(1,1),A(1,2),A(1,3)
```

```
181     CONTINUE

203     A(1,2) = NPTS
        A(1,3) = NVAR
        A(2,2) = (A(1,4/(A(1,2)-A(1,3)))**0.5
        IF(SENSE SWITCH2)869,870

869     PUNCH 5, A(2,2)
        GO TO 868

870     PRINT 5,A(2,2)

  5     FORMAT(/30H STANDARD ESTIMATE OF ERROR = E14.8//)

868     IF (SENSE SWITCH 1)889,898

202     FORMAT (E13.5,E13.5,E13.5,E13.5,E13.5)
        END
```

APPENDIX G

COMPUTER PROGRAM-CALCULATION OF R_O, R_T, Q(CORRECTED), THERMAL CONDUCTIVITY K_L, AND MAXIMUM UNCERTAINTY FROM OBSERVED DATA

```
      DIMENSION EMF(6),TEM(4),DT(4),Q(12),EME(6)
  100 FORMAT(I3,F5.0,F3.0,8F7.0)
  101 FORMAT(6F7.0,2F6.0)
  102 FORMAT(2I1)
  103 FORMAT(E13.6)
  104 FORMAT(1X,5HIC=  I1,4X,5H RO= 1PE13.6)
  300 FORMAT(2X,I5,5X,6HFREQ= 1PE13.6,5X,5HDX2= 1PE13.6,5X,5HXKL= 1PE13.
     16,4X,6HCOND= 1PE13.6,4X,6HTEMP= 1PE13.6,/12X,4HT1= 1PE13.6,6X,4HT0
     2= 1PE13.6,2X,8HTEM(1)= 1PE13.6,2X,8HTEM(2)= 1PE13.6,2X,8HTEM(3)= 1
     3PE13.6,/8X,8HTEM(4)= 1PE13.6,4X,6HHPBT= 1PE13.6,4X,6HCPLT= 1PE13.6
     4,4X,6HHPTT= 1PE13.6,4X,6HTPGT= 1PE13.6,/10X,6HHPGT= 1PE13.6,4X,6HC
     5PGT= 1PE13.6,4X,6HQ(1)= 1PE13.6,4X,6HQ(2)= 1PE13.6,4X,6HQ(3)= 1PE1
     G3.6)
  301 FORMAT(10X,6HQ(4)= 1PE13.6,4X,6HQ(5)= 1PE13.6,4X,6HQ(6)= 1PE13.6,4
     1X,6HQ(7)= 1PE13.6,4X,6HQ(8)= 1PE13.6,/10X,6HQ(9)= 1PE13.6,3X,7HQ(1
     20)= 1PE13.6,3X7HQ(11)= 1PE13.6,6X,4HQL= 1PE13.6,/10X,6HQ1HB= 1PE13
     3.6,4X,6HQ1HW= 1PE13.6,4X,6HQCOR= 1PE13.6,6X,4HRO= 1PE13.6,6X,4HRT=
     4 1PE13.6//)
      READ(5,500)DX4
  500 FORMAT(10X,F10.2)
      WRITE(6,605)
```

```
605   FORMAT(1H1)
      RSHO=1.002112E-02
      A=32.968
      B=45.463
      C=-0.84498
      TAU=0.1000
      COSC=7.752
      AP=9.56183E-02
      ASC=0.00008864
      VF12=1.524364E-02
      COR=0.0873
      AOR=2.192308E-02
      AR=8.221156E-02
      VF34=1.942008E-02
      PID=1.095583
      C2=8.333333E-03
      CQT=0.45
      AFS=1.352627E-04
      VF56=1.0
      CPL=0.12
      ARP=0.9491
      S=1.714E-09
      READ (5,102)IC,IS
 400  READ (5,103)RO
      WRITE(6,104)IC,RO
  200 READ(5,100)IN,FREQ,GRAV,HPBF,CPLF,HPTF,TPGF,HPGF,CPGF,EMFD,EMFS
      READ(5,101)EME(1),EME(2),EME(3),EME(4),EME(5),EME(6),DX1,DX2
      HPBE=HPBF*0.001
      CPLE=CPLF*0.001
      HPTE=HPTF*0.001
      TPGE=TPGF*0.001
      HPGE=HPGF*0.001
      CPGE=CPGF*0.001
      HPBT=A+B*(HPBE/4.0)+C*(HPBE/4.0)**2
      CPLT=A+B*(CPLE/4.0)+C*(CPLE/4.0)**2
```

```
      HPTT=A+B*(HPTE/4.0)+C*(HPTE/4.0)**2
      TPGT=A+B*(TPGE/4.0)+C*(TPGE/4.0)**2
      HPGT=A+B*(HPGE/4.0)+C*(HPGE/4.0)**2
      CPGT=A+B*(CPGE/4.0)+C*(CPGE/4.0)**2
      DO310I=1,6
  310 EMF(I)=EME(I)*0.001
      CONTINUE
      TO=A+B*(EMF(6)/4.0)+C*(EMF(6)/4.0)**2
      TI=A+B*(EMF(5)/4.0)+C*(EMF(5)/4.0)**2
      DO210I=1,4
  210 TEM(I)=A+B*(EMF(I))+C*(EMF(I))**2
      CONTINUE
      DT(1)=TPGT-HPTT
      DT(2)=HPBT-CPLT
      DT(3)=((HPGT-(HPTT+HPBT)/2.0))
      DT(4)=TI-TO
      CTSC=7.752+.077*(TPGT)
      Q(1)=CTSC*(ASC*3.*(DT(1)/DX1))
      Q(2)=CTSC*((5.5760E-04)*(DT(1)/DX1))
      CAT=0.0133+0.000021*((HPTT+TPGT)/2.0)
      Q(3)=CAT*(AP*(DT(1)/DX1))
      T1=TPGT+460.0
      T2=HPTT+460.0
      Q(4)=VF12*S*((T1)**4-(T2)**4)
      Q(5)=COR*0.8314*DT(3)
      Q(6)=CAT*14.1000*DT(3)
      T3=HPGT+460.0
      T4=((HPTT+HPBT)/2.+460.0)
      Q(7)=VF34*(S*((T3**4)-(T4**4)))
      CNT=0.3190+0.00037*(((HPTT+HPBT)/2.)-32.)
      CALL TEMPT(HPGT,CPLT,HPBT,DX4,CPL,DX2,TM1,TM2,TM3,TM4,TM5,TM6,TM7,
     1TM8,TM9,DELT8,DELT9,Q(8),Q(12))
      IF(IC.NE.0)GOTO330
      Q(9)=0.0
      GOTO320
  330 Q(9)=(-3.)*(CQT*(AFS*(DT(2)/DX2)))
```

```
  320 T5=(HPBT+460.0)**4
      T6=(CPLT+460.0)**4
      Q(10)=AP*VF56*(S*(TAU*(T5-T6)))
      Q(11)=-((CPL*6.28318*DX2)*DT(4)/(0.0721))
      QL=Q(1)+Q(2)+Q(3)+Q(4)+Q(5)+Q(6)+Q(7)+Q(8)+Q(9)+Q(10)+Q(11)
      EONE=(EMFD*1.0E-06)*1003.3
      CURA=(EMFS*1.E-06)/RSNO
      RST=0.01002112+(CURA*1.2E-07)
      CURB=(EMFS*1.E-06)/RST
      RLT=0.03892+(CURA*1.2E-04)
      EH=EONE-CURB*(RLT+RST)
      QINW=CURB*EH
      QINB=QINW*3.4152
      QCOR=QINB+QL
      IC=IN
      IF(IC.NE.0)GOTO220
      RO=DT(2)/QCOR
      XKL=0.0
      GOTO230
  220 RT=DT(2)/QCOR
      XKL=DX2/((RT-RO)*0.095618)
  230 COND=(QCOR*DX2)/(DT(2)*0.095618)
      TEMP=(HPBT+CPLT)/2.0
      CALL MAXMIN(HPBT,CPLT,HPTT,TRGT,HPGT,CPGT,TO,TI,DX1,VF12,S,VF34,
     1TAU,VF56,DX2,TM1,EMFD,EMFS,RSNO,CONDMX,CONDMN)
      CONDDF=CONDMX-CONDMN
      WRITE(6,610)COND,CONDMX,CONDMN,CONDDF
  610   FORMAT(1X/1X,6HCOND= ,1PE13.6,4X,10HCOND MAX= ,1PE13.6,4X,10HCOND
     1MIN= ,1PE13.6,4X,19HCOND MAX-COND MIN= ,1PE13.6)
      WRITE(6,350)DT(1),DT(2),DT(3),T1,T2,T3,T4,T5,T6,CWT,EONE,CURA,RST,
     1CURB,RLT,EH
  350 FORMAT(1HO,8X,7HDT(1)= 1PE13.6,4X,7HDT(2)= 1PE13.6,4X,7HDT(3)= 1PE
     113.6,31X,4HT1= 1PE13.6/12X,4HT2= 1PE13.6,7X,4HT3= 1PE13.6,7X,4HT4=
     2 1PE13.6,7X,4HT5= 1PE13.6,7X,4HT6= 1PE13.6/11X,5HCWT= 1PE13.6,5X,6
```

```
     3HEONE= 1PE13.6,5X,6HCURA= 1PE13.6,6X,5HRST= 1PE13.6,5X,6HCURB= 1PE
     413.6/11X,5HRLT= 1PE13.6,7X,4HEH= 1PE13.6///)
      WRITE(6,300)IN,FREQ,DX2,XKL,COND,TEMP,T1,TO,TEM(1),TEM(2),TEM(3),T
     1EM(4),HPBT,CPLT,HPTT,TPGT,HPGT,CPGT,Q(1),Q(2),Q(3)
      WRITE(6,301)Q(4),Q(5),Q(6),Q(7),Q(8),Q(9),Q(10),Q(11),QL,QINB,QINW
     1,QCOR,RO,RT
      WRITE(6,600)TM1,TM2,TM3,TM4,TM5,TM6,TM7,TM8,TM9,DELT8,DELT9,Q(12)
600   FORMAT(11X,5HTM1= 1PE13.6,6X,5HTM2= 1PE13.6,6X,5HTM3= 1PE13.6,6X,
     15HTM4= 1PE13.6,6X,5HTM5= 1PE13.6/11X,5HTM6= 1PE13.6,6X,5HTM7= 1PE1
     23.6,6X,5HTM8= 1PE13.6,6X,5HTM9= 1PE13.6,4X,7HDELT8= 1PE13.6/9X,7HD
     3ELT9= 1PE13.6,4X,7HQ(12)= 1PE13.6///)
      IF (IS.EQ.0)GOTO400
      GOTO200
      END
$IBFTC TMP
      SOBROUTINE TEMPT(TM,TC,TH,DX,CPL,DX2,T1,T2,T3,T4,T5,T6,T7,T8,T9,
     1DELT8,DELT9,Q8,Q12)
      IF(DX.GT..6)GOTO5
      TD6=TH
      IF(DX.GT..4)GOTO1
      TD4=TH
      IF(DX.GT..2)GOTO2
      TD2=TH
      GOTO3
1     TD4=TC+4.0*(TH-TC)/(DX*10.)
2     TD2=TC+2.0*(TH-TC)/(DX*10.)
3     T1P=TC+1.0*(TM-TC)/4.0
      T2P=TC+2.0*(TM-TC)/4.0
      T3P=TC+3.0*(TM-TC)/4.0
      T5=.25*(TM+T2P+TC+TD4)
      T1=.25*(TM+TM+T3P+T5)
      T3=.25*(TM+TM+T5+TD4)
      T7=.25*(T5+T1P+TC+TC)
      T9=.25*(TD4+T5+TC+TC)
```

```
      T2=.25*(TM+T1+T5+T3)
      T4=.25*(T1+T2P+T7+T5)
      T8=.25*(T5+T7+TC+T9)
      T6=.25*(T3+T5+T9+TD4)
      IC=0
4     T5S=T5
      T5=.25*(T2+T4+T8+T6)
      T3=.25*(TM+T2+T6+TD6)
      T1=.25*(TM+T3P+T4+T2)
      T7=.25*(T4+T1P+TC+T8)
      T9=.25*(T6+T8+TC+TD2)
      T2=.25*(TM+T1+T5+T3)
      T4=.25*(T1+T2P+T7+T5)
      T8=.25*(T5+T7+TC+T9)
      T6=.25*(T3+T5+T9+TD4)
      IF(ABS(T5S-T5).LT.1.0)GOTO6
      IC=IC+1
      IF(IC.LE.10)GOTO4
      WRITE(6,600)
600   FORMAT(1H1,51HTHE VALUES OF T DO NOT CONVERGE WITH 10 ITERATIONS.)
      STOP
6     DELT8=TD6-T1
      DELT9=TD2-T7
      IF(DX.EQ..3)DELT8=TD4-T4
      IF(DX.LE..2)DELT8=DELT9
      Q8=0.12*0.0044*DELT8
      Q12=(CPL*6.283*DX2*DELT9)/0.0721
      RETURN
5     WRITE(6,601)
601   FORMAT(1H1,18HDX GREATER THAN .6)
      STOP
      END
$IBFTC ERROR
      SUBROUTINE MAXMIN(HPBT,CPLT,HPTT,TPGT,HPGT,CPGT,TO,T1,DX1,VF12,S,
```

```
1VF34,TAU,VF56,DX2,TM1,EMFD,EMFS,RSMO,CONDMX,CONDMN)
 DIMENSION DTMN(4),DTMX(4),QMN(12),QMX(12)
 HPBTMN=HPBT-.01
 HPBTMX=HPBT+.01
 CPLTMN=CPLT-.01
 CPLTMX=CPLT+.01
 HPTTMN=HPTT-.04
 HPTTMX=HPTT+.04
 TPGTMN=TPGT-.04
 TPGTMX=TPGT+.04
 HPGTMN=HPGT-.04
 HPGTMX=HPGT+.04
 CPGTMN=CPGT-.04
 CPGTMX=CPGT+.04
 TOMN=TO-.04
 TOMX=TO+.04
 TIMN=TI-.04
 TIMX=TI+.04
 DTMN(1)=TPGTMN-HPTTMX
 DTMX(1)=TPGTMX-HPTTMN
 DTMN(2)=HPBTMN-CPLTMX
 DTMX(2)=HPBTMX-CPLTMN
 DTMN(3)=HPGTMN-(HPTTMX+HPBTMX)/2.0
 DTMX(3)=HPGTMX-(HPTTMN+HPBTMN)/2.0
 DTMN(4)=TIMN-TOMX
 DTMX(4)=TIMX-TOMN
 CTSCMN=7.75-0.01+0.077*TPGTMN
 CTSCMX=7.75+0.01+0.077*TPGTMX
 ASCMN=0.00008864-0.00000001
 ASCMX=0.00008864+0.00000001
 DX1MN=DX1-0.0017
 DX1MX=DX1+0.0017
 AMN   =CTSCMN*ASCMN*3.0/DX1MX
```

```
AMX   =CTSCMX*ASCMX*3.0/DX1MN
CALL TEST(AMN,AMX,DTMN(1),DTMX(1),QMN(1),QMX(1))
AMN=CTSCMN*5.5760E-04/DX1MX
AMX=CTSCMX*5.5760E-04/DX1MN
CALL TEST(AMN,AMX,DTMN(1),DTMX(1),QMN(2),QMX(2))
CATMN=0.0133-0.0001+0.000021*((HPTTMN+TPGTMN)/2.0)
CATMX=0.0133+0.0001+0.000021*((HPTTMX+TPGTMX)/2.0)
APMN=0.0956183-0.0000438
APMX=0.0956183+0.0000438
AMN=CATMN*APMN/DX1MX
AMX=CATMX*APMX/DX1MN
CALL TEST(AMN,AMX,DTMN(1),DTMX(1),QMN(3),QMX(3))
T1MN=TPGTMN+460.0
T1MX=TPGTMX+460.0
T2MN=HPTTMN+460.0
T2MX=HPTTMX+460.0
QMN(4)=VF12*S*(T1MN**4-T2MX**4)
QMX(4)=VF12*S*(T1MX**4-T2MN**4)
CORMN=0.0873-0.001
CORMX=0.0873+0.001
CALL TEST(CORMN,CORMX,DTMN(3),DTMX(3),QMN(5),QMX(5))
QMN(5)=QMN(5)*0.8314
QMX(5)=QMX(5)*0.8314
CALL TEST(CATMN,CATMX,DTMN(3),DTMX(3),QMN(6),QMX(6))
QMN(6)=QMN(6)*14.1
QMX(6)=QMX(6)*14.1
T3MN=HPGTMN+460.0
T3MX=HPGTMX+460.0
T4MN=(HPTTMN+HPBTMN)/2.0+460.0
T4MX=(HPTTMX+HPBTMX)/2.0+460.0
QMN(7)=VF34*S*(T3MN**4-T4MX**4)
QMX(7)=VF34*S*(T3MX**4-T4MN**4)
CWTMN=0.319-0.001+0.00037*((HPTTMN+HPBTMN)/2.0-32.0)
```

```
CWTMX=0.319+0.001+0.00037*((HPTTMX+HPBTMX)/2.0-32.0)
TD6MN=HPBTMN
TD6MX=HPBTMX
TM1MN=TM1-2.0
TM1MX=TM1+2.0
DELT6N=TD6MN-TM1MX
DELT6X=TD6MX-TM1MN
QMN(8)=0.12*0.0044*DELT6N
QMX(8)=0.12*0.0044*DELT6X
CQTMN=0.45-0.01
CQTMX=0.45+0.01
AFSMN=0.0001352627-0.00008
AFSMX=0.0001352627+0.00008
DX2MN=DX2-0.00004
DX2MX=DX2+0.00004
AMN=3.0*CQTMN*AFSMN/DX2MX
AMX=5.0*CQTMX*AFSMX/DX2MN
CALL TEST(AMN,AMX,DTMN(2),DTMX(2),CMN,CMX)
QMN(9)=-CMX
QMX(9)=-CMN
T5MN=(HPBTMN+460.0)**4
T5MX=(HPBTMX+460.0)**4
T6MN=(CPLTMN+460.0)**4
T6MX=(CPLTMX+460.0)**4
QMN(10)=VF56*S*TAU*(APMN*T5MN-APMX*T6MX)
QMX(10)=VF56*S*TAU*(APMX*T5MX-APMN*T6MN)
CPLMN=0.12-0.01
CPLMX=0.12+0.01
AMN=CPLMN*6.28318*DX2MN/0.0721
AMX=CPLMX*6.28318*DX2MX/0.0721
CALL TEST(AMN,AMX,DTMN(4),DTMX(4),CMN,CMX)
QMN(11)=-CMX
QMX(11)=-CMN
QLMN=QMN(1)+QMN(2)+QMN(3)+QMN(4)+QMN(5)+QMN(6)+QMN(7)+QMN(8)+
```

```
     1QMN(9)+QMN(10)+QMN(11)
      QLMX=QMX(1)+QMX(2)+QMX(3)+QMX(4)+QMX(5)+QMX(6)+QMX(7)+QMX(8)+
     1QMX(9)+QMX(10)+QMX(11)
      EMFDMN=EMFD-0.1
      EMFDMX=EMFD+0.1
      EONEMN=EMFDMN*1.0E-6*1003.3
      EONEMX=EMFDMX*1.0E-6*1003.3
      EMFSMN=EMFS-0.1
      EMFSMX=EMFS+0.1
      RSHOMN=RSHO-0.00001
      RSHOMX=RSHO+0.00001
      CURAMN=EMFSMN*1.0E-06/RSHOMX
      CURAMX=EMFSMX*1.0E-06/RSHOMN
      RSTMN=0.01002112+(CURAMN*1.2E-07)
      RSTMX=0.01002112+(CURAMX*1.2E-07)
      CURBMN=EMFSMN*1.0E-06/RSTMX
      CURBMX=EMFSMX*1.0E-06/RSTMN
      RLTMN=0.03892-0.00001+CURAMN*1.2E-04
      RLTMX=0.03892+0.00001+CURAMX*1.2E-04
      EHMN=EONEMN-CURBMX*(RLTMX+RSTMX)
      EHMX=EONEMX-CURBMN*(RLTMN+RSTMN)
      CALL TEST(CURBMN,CURBMX,EHMN,EHMX,Q1NWMN,Q1NWMX)
      Q1NBMN=Q1NWMN*3.4152
      Q1NBMX=Q1NWMX*3.4152
      QCORMN=Q1NBMN+QLMN
      QCORMX=Q1NBMX+QLMX
      AMX=QCORMX*DX2MX/0.095618
      AMN=QCORMN*DX2MN/0.095618
      BMN=1.0/DTMX(2)
      BMX=1.0/DTMN(2)
      CALL TEST(AMN,AMX,BMN,BMX,CONDMN,CONDMX)
600   FORMAT(7(1X,1PE13.6))
      RETURN
      END
```

VITA

Paul William Montgomery

Candidate for the Degree of

Doctor of Philosophy

Thesis: A STUDY OF THE EFFECT OF SINUSOIDAL VIBRATIONS UPON THE MEASUREMENT OF THERMAL CONDUCTIVITY OF DISTILLED WATER

Major Field: Mechanical Engineering

Biographical:

Personal Data: Born in Bristow, Oklahoma, August 23, 1923, the son of Walter and Nellie Montgomery.

Education: Graduated from Bristow High School, Bristow, Oklahoma, 1941; received the Bachelor of Science Degree in Mechanical Engineering from Wichita State University, Wichita, Kansas, in May, 1960; received the Master of Science Degree in Mechanical Engineering from Oklahoma State University in May, 1963; completed requirements for the Doctor of Philosophy Degree in July, 1968.

Professional Experience: Nineteen years as a navigator in the United States Air Force and currently performing duty as a Lieutenant Colonel with the regular Air Force. Present position is Deputy Director of the Aerospace Power Division, Aero Propulsion Laboratory, Wright-Patterson AFB, Ohio 45433.